

*Citation for published version:*

Darnell, R, Nakatani, Y, Knottenbelt, M, Gebhard, S & Cook, GM 2019, 'Functional characterization of BcrR: a one-component transmembrane signal transduction system for bacitracin resistance', *Microbiology*, vol. 165, no. 4, pp. 475-487. <https://doi.org/10.1099/mic.0.000781>

*DOI:*

[10.1099/mic.0.000781](https://doi.org/10.1099/mic.0.000781)

*Publication date:*

2019

*Document Version*

Peer reviewed version

[Link to publication](#)

© R. Darnell, Y. Nakatani, M. Knottenbelt, S. Gebhard, and G. Cook, 2019. The definitive peer reviewed, edited version of this article is published in *Microbiology*, Volume 165, 2019, DOI 10.1099/mic.0.000781

**University of Bath**

## **Alternative formats**

If you require this document in an alternative format, please contact:  
[openaccess@bath.ac.uk](mailto:openaccess@bath.ac.uk)

### **General rights**

Copyright and moral rights for the publications made accessible in the public portal are retained by the authors and/or other copyright owners and it is a condition of accessing publications that users recognise and abide by the legal requirements associated with these rights.

### **Take down policy**

If you believe that this document breaches copyright please contact us providing details, and we will remove access to the work immediately and investigate your claim.

1 **Revised Ms. No. MIC-D-18-00158**

2 **Functional Characterisation of BcrR: A One-Component Transmembrane**  
3 **Signal Transduction System for Bacitracin Resistance**

4  
5 **Rachel L. Darnell<sup>1,2</sup>, Yoshio Nakatani<sup>1,2</sup>, Melanie K Knottenbelt<sup>1</sup>, Susanne**  
6 **Gebhard<sup>3</sup>, and Gregory M. Cook<sup>1,2\*</sup>**

7  
8 <sup>1</sup>Department of Microbiology and Immunology, University of Otago, Dunedin, New  
9 Zealand

10 <sup>2</sup>Maurice Wilkins Centre for Molecular Biodiscovery, The University of Auckland,  
11 Private Bag 92019, Auckland 1042, New Zealand

12 <sup>3</sup>Milner Centre for Evolution, Department of Biology and Biochemistry, University of  
13 Bath, UK

14  
15 For correspondence (Gregory M Cook) Email: greg.cook@otago.ac.nz; Tel: +64 3  
16 4797722

17  
18 **Keywords:** *Enterococcus*, antimicrobial resistance, membrane protein, regulator

19 **Subject category:** Regulation

20 **Word Count:** 5,433<sup>i</sup>

21  

---

<sup>i</sup> Abbreviations: ABC ATP-binding cassette; DDM *n*-dodecyl- $\beta$ -D-maltoside, EMSA electrophoretic mobility shift assays; GOF gain of function; HA hydroxylamine hydrochloride; *lacZ*  $\beta$ -galactosidase; LB lysogeny broth; LOF loss of function; *luxABCDE* luciferase; MUG 4-methylumbelliferyl  $\beta$ -D-galactoside; NC negative control; P<sub>bcrA</sub> bcrA promoter; WT wild-type

## Abstract

Bacitracin is a cell wall targeting antimicrobial with clinical and agricultural applications. With the growing mismatch between antimicrobial resistance and development, it is essential we understand the molecular mechanisms of resistance in order to prioritise and generate new effective antimicrobials. BcrR is a unique membrane-bound one-component system that regulates high-level bacitracin resistance in *Enterococcus faecalis*. In the presence of bacitracin, BcrR activates transcription of the *bcrABD* operon conferring resistance through a putative ATP-binding cassette (ABC) transporter (BcrAB). BcrR has three putative functional domains, a N-terminal helix-turn-helix DNA-binding domain, an intermediate oligomerisation domain, and a C-terminal transmembrane domain. However, the molecular mechanisms of signal transduction remain unknown. Random mutagenesis of *bcrR* was performed to generate loss and gain of function mutants using transcriptional reporters fused to the target promoter  $P_{bcrA}$ . Fifteen unique mutants were isolated across all three proposed functional domains, comprising fourteen loss of function and one gain of function. The gain of function variant (G64D) mapped to the putative dimerisation domain of BcrR, and functional analyses indicated that the G64D mutant constitutively expresses the  $P_{bcrA}$ -*luxABCDE* reporter. DNA-binding and membrane insertion were not affected in the five mutants chosen for further characterisation. Homology modelling revealed putative roles for two key residues (R11 and S33) in BcrR activation. Here we present a new model of BcrR activation and signal transduction, providing valuable insight into the functional characterisation of membrane-bound one-component systems and how they can co-ordinate critical bacterial responses, such as antimicrobial resistance.

## INTRODUCTION

One-component regulatory systems containing both a sensory domain and DNA-binding domain dominate signal transduction systems in bacteria and archaea [1]. They regulate important cellular functions such as antimicrobial resistance, metal homeostasis, carbon and amino acid metabolism, and quorum sensing [2]. They are both evolutionarily older and more widely distributed than their two-component counterparts [1, 2]. However, they are vastly understudied, particularly those that are membrane-bound [1].

BcrR is a unique one-component regulator of high-level zinc-bacitracin (bacitracin) resistance in *Enterococcus faecalis* [3]. BcrR consists of three proposed functional domains, a N-terminal helix-turn-helix (HTH) DNA-binding domain, an intermediate oligomerisation domain and a C-terminal transmembrane domain [4]. We have previously shown BcrR directly detects bacitracin *in vitro* [5]. Intrinsic tryptophan fluorescence of BcrR was reduced in the presence of bacitracin, suggesting a direct interaction between BcrR and bacitracin [5]. Previous electrophoretic mobility shift assays (EMSAs) and  $P_{bcrA}$ -*lacZ* reporter assays have shown that BcrR is constitutively bound to two sets of inverted DNA repeat sequences upstream of its resistance operon, *bcrABD*, but requires bacitracin for activation [4]. BcrR is therefore thought to exist as dimers in its inactive state, with oligomerisation (likely dimer-dimer formation) induced upon addition of bacitracin. The DNA-binding footprint of BcrR on the *bcrABD* promoter region does not change between induced and uninduced states, suggesting a conformational change in BcrR, and/or subtle changes in local DNA topology are required to initiate *bcrABD* expression [5]. How BcrR binds bacitracin and transduces the signal to initiate *bcrABD* expression remains unknown.

The first two genes in the target operon, *bcrAB*, encode a putative heterodimeric ABC efflux transporter (BcrAB) that is essential for high-level bacitracin resistance [3]. This transporter is distinct from other ABC transporters (i.e. BceAB) that are frequently associated with drug removal in Firmicute bacteria, such as *Enterococcus* and *Bacillus* [3, 6–8], in that its expression is regulated by a one-component rather than two-component system [8–10]. The third target gene, *bcrD*, encodes an uncharacterised undecaprenyl pyrophosphate phosphatase that is not necessary for high-level resistance [3].

The aim of this study was to identify key residues critical for BcrR function using random mutagenesis and reporter assays, to further our understanding of the role these three functional domains play in one-component signal transduction systems. Fifteen unique mutations were identified, fourteen loss of function (LOF) and one gain of function (GOF). The G64D GOF mutant was localised to the putative dimerisation domain of BcrR. The transcription activation profile of the GOF G64D mutant was determined using the  $P_{bcrA}$ -*luxABCDE* reporter in order to understand its ability to activate *bcrABD* in the absence of the inducer, bacitracin. A further four mutants (in addition to G64D) spanning all three functional domains were chosen for detailed characterisation of cellular localisation and DNA-binding capability. A three-dimensional model was constructed of the DNA-binding domain (DBD) to further elucidate the role of the DBD mutants in BcrR function.

## METHODS

### Bacterial strains and growth conditions

All strains used in this study are listed in Table S1, the *Bacillus subtilis* SGB37 strain was used as a heterologous host for transformation and expression of mutant *bcrR*,

and BcrR activity assays. Genomic DNA was isolated from the *E. faecalis* strain AR01/DGVS and used as a template for PCR amplification of *bcrR*. *Escherichia coli* strains DH10B and C41(DE3) were used for cloning and protein production, respectively. *E. coli* and *B. subtilis* were routinely grown in lysogenic broth (LB) media at 37°C overnight (200 r.p.m), while *E. faecalis* was grown in brain heart infusion (BHI) media at 37°C with no agitation. For protein production, *E. coli* C41(DE3) was grown in 2 × yeast extract and tryptone (2 × YT) at 37°C (200 r.p.m), unless otherwise stated. *B. subtilis* was transformed by natural competence as previously described [11]. Selective media contained ampicillin (amp; 100 µg ml<sup>-1</sup> for *E. coli*), chloramphenicol (cm; 5 µg ml<sup>-1</sup> for *B. subtilis*), kanamycin (kan; 10 µg ml<sup>-1</sup> for *B. subtilis*), and spectinomycin (spec; 100 µg ml<sup>-1</sup> for *B. subtilis*), where required. Bacitracin (bac; 0.5 µg ml<sup>-1</sup> for *B. subtilis*), xylose (xyl; 0.2% (w/v) for *B. subtilis*), and 5-bromo-4-chloro-3-indolyl β-D-galactopyranoside (X-gal; 100 µg ml<sup>-1</sup> for *B. subtilis*) were added to LB agar to select for LOF and GOF *bcrR* mutants. All solid media contained 1.5% (w/v) agar. Growth was measured as an optical density at 600 nm (OD<sub>600</sub>) (Jenway 6300 Spectrophotometer).

### Hydroxylamine mutagenesis of *bcrR*

Full length *bcrR* was previously cloned into the xylose-inducible plasmid pES701 (pXT-*bcrR*) (Table S1) [12]. The pXT-*bcrR* plasmid was randomly mutagenised by incubation with the chemical mutagen hydroxylamine hydrochloride (HA) (1.25 mg per µg of DNA) in sodium phosphate buffer (f/c 50 mM sodium phosphate pH 7.0, 100 mM NaCl, 25 mM EDTA) at 75°C for 15 min (Fig. 1). Mutated pXT-*bcrR* (mut*bcrR*) plasmid was purified by gel electrophoresis purification using the illustra™ GFX™ PCR DNA and gel band purification kit (GE Healthcare) (Table S1). The plasmid mut*bcrR* was used to transform *B. subtilis* strain SGB37 (harbouring P<sub>bcrA</sub>-*lacZ*) and *B. subtilis* strain

SGB273 (harbouring  $P_{bcrA}$ -*luxABCDE*), plated on LB<sub>spec</sub> agar and screened for LOF or GOF [11].

### **Isolation of LOF and GOF *bcrR* mutants**

A modified protocol of traditional blue-white screening was used to isolate colonies with BcrR LOF or GOF [12]. LOF mutants were identified as white colonies on LB<sub>bac, xyl, Xgal</sub> agar plates (i.e. white = LOF), due to their inability to produce active BcrR, and are therefore unable to initiate expression of the  $\beta$ -galactosidase reporter construct  $P_{bcrA}$ -*lacZ* (Fig. 1 and Fig. S1). GOF mutants were identified as blue colonies on LB<sub>xyl/Xgal</sub> plates, due to their ability to produce active BcrR in the absence of its inducer (bacitracin) and subsequently initiate expression of the  $\beta$ -galactosidase (Fig. 1 and Fig. S1). GOF mutants were also identified as luminescing colonies on LB<sub>xyl</sub> agar plates in a SGB273 background. Mutations in putative LOF and GOF mutants were verified by DNA sequencing using the primer pair pXT-check fwd and pXT-check rev (Table S2).

### **$\beta$ -galactosidase and luciferase assays**

$\beta$ -galactosidase assays using the fluorogenic substrate 4-methylumbelliferyl  $\beta$ -D-galactoside (MUG) were carried out on all integrative *lacZ* reporter strains to quantitatively verify BcrR loss and gain of function phenotypes. BcrR mutant and control strains were grown to an OD<sub>600</sub> of 0.4 in LB broth containing 0.2% xylose. Samples (100  $\mu$ l) were taken and placed in four wells of a 96-well microtitre plate for each replicate of each strain. Cultures were challenged with 0, 0.1, 0.5, and 1  $\mu$ g ml<sup>-1</sup> of bacitracin for 1 h. Cell density was determined as a final OD<sub>600</sub> using the Varioskan Flash Multimode Reader (Thermo Fisher Scientific) and plates were subsequently frozen at - 80°C. Expression analysis was measured as previously described [12, 13].

An unpaired *t*-test was performed between the wild-type (WT) and vector control (NC), along with the WT and BcrR mutants at 1 µg ml<sup>-1</sup> bacitracin to determine statistical significance of respective β-galactosidase activities (an adjusted *p* value of ≤ 0.05).

Luciferase activities of WT and G64D mutant BcrR were assayed using a Varioskan Flash Multimode Reader (Thermo Fisher Scientific) as previously described, with the following modifications [12]. Cultures were grown in the presence or absence of xylose (0.2%) to an OD<sub>600</sub> of 0.1 and plated onto a 96-well microtitre plate. Cultures were challenged with final bacitracin concentrations of 0, 0.1, 0.5, and 1 µg ml<sup>-1</sup> for 2 h, with OD<sub>600</sub> and luminescence measured every 20 min.

### **Generation of wild-type and mutant BcrR protein expression constructs**

Wild-type BcrR and five BcrR mutants (R11K, S33L, G64D, E179K, and T183M) were selected for further investigation. BcrRFwd and HisBcrRRev primers were used to clone WT *bcrR* from *E. faecalis* strain AR01/DGVS into the IPTG-inducible expression vector pTrc99A to produce pBcrRHis<sup>WT</sup> (Table S1 and S2). A His<sub>6</sub> tag was introduced at the C-terminus of BcrR for purification purposes. Respective mutations for each selected mutant were introduced into WT *bcrR* using site-directed mutagenesis and overlap extension PCR to create the five BcrR variants pBcrRHis<sup>R11K</sup>, pBcrRHis<sup>S33L</sup>, pBcrRHis<sup>G64D</sup>, pBcrRHis<sup>E179K</sup>, pBcrRHis<sup>T183M</sup> (Tables S1 and S2) [14]. Constructs were confirmed by DNA sequencing. Chemically competent *E. coli* C41(DE3) were transformed (by heat-shock) with pBcrRHis<sup>WT</sup> and mutant plasmids, to generate strains WT, R11K, S33L, G64D, E179K, and T183M for protein production and purification (Table S1).

### **Cellular localisation of BcrR wild-type and mutant forms**



*E. coli* strains producing BcrR WT and BcrR mutant protein were grown in 2 × YT<sub>amp</sub> media. When cultures reached an OD<sub>600</sub> of 0.6 – 0.8 expression was induced with 1 mM IPTG and cells were grown for a further 2 h. Cells were harvested by low-speed centrifugation (15 min, 10,000 × *g* at 4°C) and resuspended in lysis buffer (50 mM Tris/HCl, 5 mM MgCl<sub>2</sub>, pH 7.5). Cells were lysed by three passages through the Aminco French Press at 40 kpsi at 4°C. Unbroken cells and debris were removed by low speed centrifugation (15 min, 10,000 × *g* at 4°C) and the cell lysate underwent high speed centrifugation (90 min, 123,695 × *g* at 4°C) to separate the membrane and cytosolic fractions. Supernatants were removed, and membrane pellets were resuspended in lysis buffer, both were stored at -20°C.

Protein concentrations in the cytoplasmic and membrane fractions were determined by DC Bradford (BioRad) using bovine serum albumin (BSA) as a standard. Protein samples (about 50 µg) of both membrane and cytoplasmic fractions were run on 12.5% SDS-PAGE gel, 125 V for 1.5 h using the Laemmli-SDS buffering system, and protein was visualised by standard silver staining [15]. Western Blot analysis was used to confirm BcrRHis WT and BcrR mutant protein was the ~20 kDa protein observed in the membrane fraction. Western Blots were carried out using a previously described protocol with an anti-His antibody (Abcam ab1187) and visualised using the Odyssey Fc Imaging System (LI-COR® Biosciences) [4].

### **Protein purification of WT and mutant BcrRHis, and reconstitution into liposomes**

All six BcrR variants underwent protein purification using a previously described method with the following modifications [4]. Overproduction of BcrR is toxic to *E. coli*, therefore to optimise protein yield, 750 ml *E. coli* cultures were grown in 2 L flasks in

2 × YT media, supplemented with ampicillin, with agitation and aeration (200 r.p.m) at 37°C [4]. At OD<sub>600</sub> 1.5 - 2, the cultures were induced with 1 mM IPTG and incubated for a further 1 h. Cells were lysed by two passages through the Constant Systems Ltd Cell Disrupter at 31 kpsi and 4°C. Membranes were stored at - 20°C for BcrR solubilisation and purification the following day. Prior to solubilisation, membranes were washed with buffer A (20 mM sodium phosphate pH 7.5, 0.1 mM PMSF, 5 mM DTT, 500 mM sodium chloride) containing 0.5% sodium cholate and disrupted by sonication (20% Amp) on ice for 6 × 30 sec cycles with 1 min rest periods. Membranes were ultra-centrifuged at 150,000 × *g* for 45 min. Membranes were then solubilised with buffer A containing 1% *n*-dodecyl-β-D-maltoside (DDM) and disrupted by sonication (as above). Solubilised protein was ultra-centrifuged at 150,000 × *g* for 45 min. The supernatant (solubilised BcrR) was stored on ice and solubilisation was repeated for optimal protein yield. The supernatant was loaded onto a Ni<sup>2+</sup> HisTrap HP column (5 ml) using an AKTA Prime Plus (GE Healthcare) pre-equilibrated with five column volumes of buffer A containing 0.5% DDM and 10% glycerol (buffer A\*). Unbound sample was removed by washing with buffer A\* and buffer B (buffer A\* containing 500 mM imidazole) at a ratio of 80:20 (at a rate of 2 ml min<sup>-1</sup>). BcrRHis was eluted (at a rate of 1 ml min<sup>-1</sup>) at a buffer A\*- buffer B ratio of 30:70 and collected in 1ml fractions. Remaining protein was eluted in 100% buffer B. In all cases elution was monitored by absorption at 280 nm in Primeview. Fractions collected from the 30:70 peak were analysed by SDS-PAGE and visualised with Coomassie G-250 (Bio-Rad) (Fig. S2. a - f). BcrR-containing fractions were pooled and placed in Snakeskin® Pleated Dialysis Tubing (3,500 MWCO) and dialysed in 100 volumes of buffer A containing 10% glycerol at 4°C overnight with gentle stirring. Dialysed protein was

analysed by SDS-PAGE and protein was quantified by DC Bradford (BioRad) using a BSA standard. Average final protein concentrations were 3.5 - 5 mg ml<sup>-1</sup>.

BcrRHis WT and mutants were reconstituted into L- $\alpha$ -phosphatidyl-choline liposomes (Sigma P5638) for electrophoretic mobility shift assays. BcrRHis WT and mutant protein was added to lipid at a ratio of 1:20 (protein:lipid), Triton X-100 and BioBeads® (BioRad) were used to integrate BcrRHis into liposomes to create BcrRHis WT, R11K, S33L, G64D, E179K, and T183M proteoliposomes using a previously reported protocol [5]. Protein concentration was quantified by separating protein from lipid on a 12.5% SDS-PAGE gel containing four times the normal amount of SDS, alongside a BSA protein standard (Fig. S3).

### **Electrophoretic Mobility Shift Assays (EMSA)**

EMSAs were used to determine DNA-binding capacity of each of the five BcrRHis variants to the *P<sub>bcrA</sub>* target promoter. *P<sub>bcrA</sub>* was amplified by PCR, using primers bcrA\_EMSA\_F and bcrA\_EMSA\_R to produce a 92 bp DNA probe. The forward primer, bcrA\_EMSA\_F was tagged at the 5' end with a 5'IRDye700 fluorophore (LI-COR® Biosciences/Integrated DNA Technologies) for visualisation at 700 nm (Table S2). Non-labelled competitor probe was amplified by PCR, using the primers bcrA\_EMSA\_F (without the IRDye700 label) and bcrA\_EMSA\_R (Table S2). Binding reactions were carried out using a previously described method with the following modifications: 1.9 ng (32 fmoles) of labelled DNA was used in all binding reactions, and reactions were carried out at molar ratios of BcrR:DNA (0:1, 25:1, 50:1, and 125:1) in the dark, at room temperature [4]. Reactions were run on pre-cooled and pre-run (120 V, 1 h) 6% native acrylamide gels (37.5:1 acrylamide:bisacrylamide) in 0.5 TBE (40 mM Tris-HCl (pH 8.3), 45 mM boric acid, 1 mM EDTA) on ice in a dark

room at 350 V for 25 min. Gels were visualised for 10 min at 700 nm using the Odyssey® Fc Imaging System (LI-COR® Biosciences) with minimum light exposure.

### **BcrR three-dimensional structural model**

A three-dimensional model of the BcrR DNA-binding domain was predicted using the P22 c2 repressor protein, which has the highest homology to BcrR (34% identity) (PDB file: 3JXB), as a model in ProtMod (Godzik Lab, The Burnham Institute). Structural analysis and amino acid substitution was carried out using PyMOL (The PyMOL Molecular Graphics System, Version 1.7 Schrödinger, LLC) [16].

## **RESULTS AND DISCUSSION**

### **Isolation and characterisation of loss and gain of function mutations in BcrR**

Loss (LOF) and gain of function (GOF) BcrR mutants were identified using *B. subtilis* strain SGB37 as a heterologous host as previously described [12]. Mutant BcrR (*mutbcrR*) was integrated into the host genome alongside the reporter for BcrR activity  $P_{bcrA}$ -*lacZ* ( $\beta$ -galactosidase), following successful transformation. LOF and GOF mutants were isolated using a modified blue-white screening protocol as previously described [12]. LOF mutants were white in the presence of bacitracin, due to their inability to activate  $P_{bcrA}$ -*lacZ* expression, while GOF mutants were identified as blue colonies in the absence of bacitracin due to their ability to activate  $P_{bcrA}$ -*lacZ* expression in the absence of bacitracin (Fig. 1 and Fig. S1).

A total of 428 colonies were screened for loss and gain of BcrR function. The average loss of function frequency was 8.3% (data not shown). All loss and gain of function mutants were sequenced to identify point mutations responsible for their respective phenotype. A total of fifteen unique *bcrR* point mutants were isolated using the  $\beta$ -galactosidase reporter (Table 1). Mapping to the BcrR protein sequence identified four

substitutions in the predicted helix-turn-helix (HTH) DNA-binding domain (DBD) motif (R11K, T17M, T30I, and S33L), four in the putative oligomerisation domain (OGD) (P42L, S51F, G64S, and G64D), and seven in the transmembrane domain (TMD) – four in the putative first and second transmembrane helices (G88R, P101L, T123I, and G141D), and three in the second extracellular loop (E179K, P180S, and T183M) (Fig. 2). A number of mutations were observed more than once, and all mutations conferred a LOF, except G64D which resulted in a GOF (Table 1). Only one GOF mutant was isolated using the luciferase reporter ( $P_{bcrA}$ -*luxABCDE*). Coincidentally, this mutant carried the same G64D substitution as the  $\beta$ -galactosidase GOF mutant.

#### **Quantitative measurement and validation of BcrR mutant activity**

BcrR activity in each of the LOF and GOF mutants was quantitatively measured using  $\beta$ -galactosidase assays (Fig. 3). Fluorescence (MUG) emitted by  $\beta$ -galactosidase activity was measured for each mutant at a range of bacitracin concentrations (0, 0.1, 0.5 and 1  $\mu\text{g ml}^{-1}$ ) and compared to the BcrR wild-type (WT) and empty vector control (NC). All strains were grown in the presence of xylose (0.2%) to ensure *bcrR* expression. WT BcrR activity ( $P_{bcrA}$ -*lacZ* expression) was dose-dependent and maximal activity was observed at 1  $\mu\text{g ml}^{-1}$  bacitracin (2000 RFU) (Fig. 3). The vector control showed a negligible response with a maximal activity of 20 RFU (Fig. 3). Thirteen of the fourteen LOF mutants from all three protein domains showed similar activity to the vector control, validating their LOF phenotype (Fig. 3). The G64S mutant displayed higher activity than the rest of the LOF mutants but remained significantly lower than WT in the presence of bacitracin, and therefore remained classified as LOF (Fig. 3b). Interestingly, the GOF mutant (G64D) was still inducible by bacitracin and expression was 3-fold higher than the WT at 1  $\mu\text{g ml}^{-1}$  bacitracin (Fig. 3b).

To validate the genomic-phenotypic linkages of the BcrR point mutations, genomic DNA (gDNA) was isolated from three LOF BcrR mutant *B. subtilis* strains (S33L, G64S, and E179K), the GOF mutant (G64D) strain, and the WT strain (SGB43) (Table 1 and Table S1) using a previously described protocol [11]. This was to provide a “clean” genetic background, and to absolve any chance the observed LOF phenotype was due to a loss of  $\beta$ -galactosidase activity, rather than the associated BcrR point mutation. Clonal cultures of the *B. subtilis*  $P_{bcrA}$ -*lacZ* reporter strain (SGB37; Table S1) were independently transformed with gDNA from each of the stated strains. Transformants were plated on LB agar containing spectinomycin to select for uptake of the BcrR construct. Three clones for each BcrR variant were streaked on LB<sub>xyl,bac,Xgal</sub> agar to phenotypically confirm BcrR function (Fig. S1). BcrR presence was detected in all clones by colony PCR. The G64D GOF mutant appeared as blue colonies, which represents activated BcrR and are darker than the light blue WT, indicating an increased activation state in the G64D mutant (Fig. S1a – b). The colonies for the LOF mutants S33L, G64S, and E179K (Fig. S1c - e), appeared white in colour, which represents a lack of active BcrR, i.e. LOF. BcrR activity was quantified for each BcrR variant by  $\beta$ -galactosidase activity analysis using the fluorogenic substrate MUG. Activity for each BcrR variant was comparable to the original assay (Fig. 3 and Fig. S4). This suggests these are indeed bona fide loss and gain of function BcrR point mutations, further supported by the independent isolation of most point mutations on more than one occasion (see “Frequency” Table 1).

#### **The bacitracin activation profile of the BcrR gain of function mutant G64D**

Two substitutions were observed at the same residue G64 (S and D), resulting in both a LOF and GOF genotype respectively. This residue is localised to the putative oligomerisation domain of BcrR, and oligomeric state is believed to play an important

role in BcrR activation [5]. The *bcrA* promoter consists of two sets of inverted repeats that are essential for BcrR binding, and BcrR is often observed in both the monomeric and dimeric form [4]. Previous findings suggest BcrR forms a tetrameric dimer-dimer complex upon activation by bacitracin, therefore we hypothesise G64 may play a critical role in the formation of this complex [4, 5]. To investigate this proposal further, we carried out a more detailed analysis of the G64D activation profile (Fig. 4).

BcrR G64D activity was compared to WT BcrR using the integrative luciferase reporter construct  $P_{bcrA}$ -*luxABCDE* in the *B. subtilis* strain SGB273. Luciferase activity was used in place of  $\beta$ -galactosidase due to its greater sensitivity to activated BcrR (as observed in the absence of bacitracin, Fig. 3b and 4a). A comparison of BcrR WT and G64D activity was carried out in the presence of xylose (0.2%) and at a range of bacitracin concentrations (0, 0.1, 0.5 and 1  $\mu\text{g ml}^{-1}$ ). BcrR G64D activity was significantly higher than WT at 0 and 0.1  $\mu\text{g ml}^{-1}$  of bacitracin (Fig. 4a and 4b), but there was no significant difference at 0.5 and 1  $\mu\text{g ml}^{-1}$  of bacitracin (Fig. 4c and 4d). We hypothesise the G64D mutation stabilises BcrR at 0 and 0.1  $\mu\text{g ml}^{-1}$  of bacitracin allowing for spontaneous activation and hyper-sensitivity upon addition of low levels of bacitracin, while WT requires bacitracin for activation. It is also likely that binding of bacitracin stabilises BcrR, and this may explain why we do not see a significant difference in G64D and WT activity at 0.5 and 1  $\mu\text{g ml}^{-1}$  of bacitracin.

In the *B. subtilis* heterologous host strains, BcrR expression in the integrative pXT-*bcrR* plasmid is under the control of a xylose-inducible promoter cloned upstream of the *bcrR* gene. However, this promoter is known to be leaky [17]. Therefore, to ensure the observed G64D phenotype was not an artefact of high BcrR expression and to mimic low-level constitutive BcrR expression as observed in its native enterococcal environment [3], luciferase assays were repeated in the absence of xylose. This

showed G64D activity was also significantly higher than WT at 0 and 0.1  $\mu\text{g ml}^{-1}$  of bacitracin, but not at 0.5 or 1  $\mu\text{g ml}^{-1}$  at low levels of BcrR expression (albeit at lower overall levels) (Fig. 5 a – d). This suggests the G64D mutation is of physiological significance for BcrR function in its native environment [3, 4].

#### **DNA-binding activity of BcrR mutants R11K, S33L, G64D, E179K and T183M**

Previous investigations have found that BcrR requires membrane localisation for DNA-binding activity and function [4, 5]. Five BcrR mutants, R11K, S33L (from the DBD), G64D (oligomerisation domain), and E179K and T183M (localised to the second extracellular loop cluster of the TMD), were chosen for further functional characterisation. To determine whether these mutations influenced the DNA-binding capability of BcrR, EMSAs were performed with the *bcrABD* target promoter region ( $P_{bcrA}$ ) (Fig. 6a). A shift of the  $P_{bcrA}$  DNA probe was observed for WT BcrR and all five BcrR mutants (Fig. 6 b – g). No shift was observed in the absence of BcrR (Fig. 6h, liposome-only control). However, auto-fluorescence of the liposomes was detected. To avoid introduction of experimental artefact, densitometric analyses were subsequently performed on the probe (Fig. 6b – g and Fig. S5). The densitometric data shows that upon addition of BcrR-containing proteoliposomes, the relative band intensity of the probe decreases (Fig. S5). In the BcrR WT and S33L mutant, this shift is concentration-dependent (Fig. S5). For the BcrR R11K, G64D, E179K, and T183M mutants, a complete band shift is observed at the lowest ratio of BcrR:DNA (25:1) (Fig. S5). A non-labelled competitor probe (of the same length and nucleotide sequence as  $^{125}\text{I}$ - $P_{bcrA}$ ) was able to displace the labelled  $P_{bcrA}$  target probe at increasing concentrations, shown as an increase in free labelled probe and a decrease in bound probe (Fig. S6a, lanes 1 – 5). This additional control, alongside previous work that has



shown BcrR proteoliposomes bind a site-specific probe [4, 5], confirms BcrR WT and all five BcrR mutants are able to specifically bind the target *bcrA* DNA probe.

### **Molecular modelling of the BcrR DNA-binding domain and theoretical analysis of the DNA-binding domain mutants**

The DBD mutants R11K and S33L were able to recognise and bind to the *bcrABD* promoter, despite conferring a loss of BcrR function. Therefore, in order to further understand the implications of the R11K and S33L substitutions on BcrR function, a three-dimensional model of the DBD was constructed. A NCBI protein BLAST of the DBD (residues 1 - 69) against the Protein Databank identified the P22 c2 phage repressor DNA-binding domain (PDB sequence file: 3JXB), meeting the criteria of well-characterised and highest sequence homology (34%) (Fig. 7a). The P22 c2 phage repressor protein structure was used as a model in ProtMod for the structural analysis of the BcrR DNA-binding domain (Fig. 7b - d) [16]. The three-dimensional model predicts that five  $\alpha$  helices make up the BcrR DBD (helices 1 - 4), with helices 2 (16 - 25) and 3 (28 - 37) forming the HTH motif, and bordering helices 1 (3 - 13) and 4 (44 - 53) providing structural support (Fig. 7a and 7b). It also suggests BcrR forms a homodimer at each set of inverted repeats and highlights a potential dimerisation interface between residues 40 - 61 (helix 4 and 5) (Fig. 7b). This observation hypothesises functional overlap between the DBD and OGD, and therefore indicates oligomeric status could play an important role in transitioning the DBD from an inactivated to activated conformational state in the presence of bacitracin.

Virtual amino acid substitutions were carried out on the three-dimensional model for R11K and S33L using PyMOL (The PyMOL Molecular Graphics System, Version 1.7 Schrödinger, LLC) (Fig. 7). An R11K substitution appears to disrupt a conserved salt

bridge between R11 (R14 in model) and E36 (E39) and eliminate the hydrogen bond between R11 and L16 (I19 in model) in the DBD model (Fig. 7c and d). The R11 residue is conserved among XRE-type HTH DNA-binding domains (R14 in P22 c2 and R10 in 434) (Fig. 7a), and previous investigations in the P22 c2 and 434 Cro repressor have shown that this residue provides structural support to the HTH motif (helices 2 and 3) through the observed salt bridge (R11 - E36) and hydrogen bond (R11 - L16) (Fig. 7c) [18, 19]. Disrupting this interaction in the 434 phage repressor (R10M) loosens the core structure of the DNA-binding domain and alters the DNA-binding surface of the protein [20]. We therefore hypothesise that a less dramatic R to K change at position 11 allows the BcrR R11K mutant to retain its ability to bind to the *bcrABD* target promoter as observed in the EMSA (Fig. 7c); but propose, loss of the hydrogen bond between R11 and L16 and weakening of the R11 - E36 salt bridge may alter the DNA-binding surface upon activation by bacitracin, thereby affecting the ability of BcrR R11K to induce transcription of the *bcrABD* operon.

The three-dimensional model predicts a S33L (S36 in model) substitution disrupts the direct hydrogen bond with the DNA phosphate oxygen due to the lack of a polar hydroxyl side group (Fig. 7c and d), which would suggest the loss of function in the S33L is likely due to inability to bind to the target promoter. However, the EMSAs show S33L retains its ability to bind and recognise the target promoter (Fig. 6d). We therefore hypothesise that some interactions at the protein and DNA interface are essential for constitutive binding to the DNA promoter, while others are essential for transducing bacitracin-dependent activation to the DNA promoter to allow initiation of transcription of *bcrABD* by RNA polymerase (RNAP).

The mechanism of promoter activation by BcrR is unknown, however it is thought that upon binding of bacitracin BcrR undergoes a conformational change. This is thought

to result in either a topological change in the *bcrABD* promoter exposing the core promoter elements to RNAP, or in recruitment of RNAP by the promoter-proximal dimer of BcrR [5]. Low-affinity protein-DNA operator complexes have previously been shown to reduce DNA-twisting [18, 21] therefore, it is conceivable that in the absence of either the R11 - L16 hydrogen bond, or the S33 - DNA hydrogen bond, BcrR is unable to transduce the signal from the bacitracin-binding site to the target promoter to allow exposure of the core promoter elements, and initiation of *bcrABD* expression.

### **BcrR localisation to the cell membrane**

Membrane localisation is essential for BcrR function and therefore mutations in the transmembrane domain that confer a LOF likely result in a misfolded protein that is either displaced from the membrane, subjected to degradation, or insensitive to bacitracin. Two transmembrane domain mutants E179K and T183M were tested for cellular localisation, using BcrR WT and three mutants R11K, S33L, and G64D as controls. For these experiments, BcrR WT and mutants were expressed in *E. coli* as we have previously shown that functional BcrR localises to the membrane in this bacterium [4] and non-functional BcrR (membrane domain removed) localises to the cytoplasm [5]. Upon expression of BcrR WT and variants in *E. coli* cellular proteins were subsequently separated into membrane and cytosolic fractions. Fractions were analysed by SDS-PAGE and BcrR localisation probed by Western Blot (Fig. 8a and b). When the membrane fractions were run alongside the cytosolic (supernatant after ultracentrifugation) fraction, BcrR was clearly observed in the membrane fraction, and not in the cytosolic fraction (Fig. 8a). BcrR was found in the membrane fraction in all cases, confirming that membrane localisation does not play a role in either of the loss or gain of function BcrR mutants.

BcrR is reported to directly detect bacitracin, but the bacitracin-binding site of BcrR has not been identified [5]. Transmembrane receptor proteins such as sensor kinases ApsS and PhoQ, which regulate resistance to cationic antimicrobial peptides (CAMPs), are known to detect target ligands through their extracellular domains [22–24]. These proteins sense CAMPs at the membrane surface through an acidic extracellular loop that can vary in length from nine amino acids in ApsS to 145 in PhoQ, and while bacitracin is not a CAMP, it does have amphipathic properties [24, 25]. BcrR has two putative extracellular loops embedded in its C-terminal transmembrane domain. Seven LOF mutations were isolated in the TMD, with three (E179K, P180S, and T183M) clustered to the second extracellular loop. We have previously shown direct bacitracin-binding using tryptophan fluorescence, however this technique lacked the sensitivity to detect differences between WT and these LOF mutants (data not shown). Nevertheless, we hypothesise the second extracellular loop of the transmembrane domain may serve as a potential bacitracin-binding site, exploiting the hydrophilic and hydrophobic properties of this region to aid in binding of the amphipathic bacitracin.

AgrC binds its target peptide through a two-step process which involves initial non-specific interactions in the hydrophobic pocket formed by the transmembrane helices, followed by specific hydrophilic interactions provided by the final extracellular loop [26, 27]. We hypothesise bacitracin binding may trigger conformational changes that are transduced to the DNA-binding domain, via the oligomerisation domain that activate BcrR. As the protein is constitutively bound to its target DNA, these conformational changes are then thought to change the local DNA topology and/or mediate direct interactions with RNAP [4, 5], leading to expression of *bcrABD* and ultimately activation of bacitracin resistance.

## Conclusion

We originally identified the *bcr* locus in a bacitracin-resistant clinical isolate of *E. faecalis* using a transposon mutagenesis screen, which has since been identified in other Gram-positive bacteria, such as *Clostridium perfringens* [3, 28]. Acquired bacitracin resistance in *E. faecalis* is mediated by an ABC transporter (BcrAB) and a novel regulatory protein, BcrR [3]. Here, we have carried out random mutagenesis on the high-level bacitracin resistance regulator BcrR to further our understanding of how it functions as a membrane-bound one-component system. Fifteen unique point mutations were identified in *bcrR*, distributed across all three putative functional domains, the N-terminal XRE-type DNA-binding domain, intermediate oligomerisation domain, and C-terminal transmembrane domain. Of these fifteen mutations, fourteen conferred a loss of BcrR function, and one a hyper-sensitive GOF. Previous work has established *B. subtilis* and *E. coli* as heterologous hosts for analysis of BcrR function and we employed these systems here for further analysis of five BcrR mutants [4, 5, 12]. Two mutants were identified at the G64 locus, a G64S substitution that significantly reduced bacitracin-induced BcrR activation and a G64D substitution that significantly increased activation compared to the WT. This G64D substitution also allowed BcrR activation in the absence of bacitracin under xylose-inducible expression. We propose a model that suggests the presence of glycine at position 64 plays a critical role in regulating BcrR activation, thereby allowing expression of the resistance operon *bcrABD* only in the presence of bacitracin (Fig. S7). We hypothesise that this may also explain why even subtle substitutions such as G64S significantly alter BcrR activity (Fig 3b). Promoter activity assays were utilised to analyse transcription activation of the G64D gain of function mutant. They highlighted the importance of the oligomerisation domain- specifically G64 in regulating BcrR

activation in the presence of bacitracin (Fig. S7 and Fig. 9). We showed that the DNA-binding domain is not only important for binding the *bcrABD* promoter, but also for transducing and activating BcrR in the presence of bacitracin to allow initiation of *bcrABD* transcription by RNAP; and identified a potential bacitracin-binding site localised to a cluster of BcrR loss of function mutants at the second extracellular loop in the transmembrane domain (Fig. 9). BcrR was the first membrane-bound one-component high-level antimicrobial resistance regulator identified in bacteria. This work builds on our previous work as it highlights the essentiality of each functional domain, and their co-operation, in order to articulate an effective response.

## Acknowledgements

We would like to thank Christoph von Ballmoos and Linda Naesvik Oejemyr for their expert advice, and Rob Fagerlund for his technical assistance. This work was supported by a University of Otago PhD Scholarship and Publishing Bursary (R.L.D.), the Todd Foundation of New Zealand Excellence Scholarship (R.L.D.), and the Deutsche Forschungsgemeinschaft (DFG; grant GE2164/3-1) (S.G.).

We declare no conflict of interest.

## Abbreviations

ABC ATP-binding cassette; DDM *n*-dodecyl- $\beta$ -D-maltoside, EMSA electrophoretic mobility shift assays; GOF gain of function; HA hydroxylamine hydrochloride; *lacZ*  $\beta$ -galactosidase; LB lysogeny broth; LOF loss of function; *luxABCDE* luciferase; MUG 4-methylumbelliferyl  $\beta$ -D-galactoside; NC negative control;  $P_{bcrA}$  *bcrA* promoter; WT wild-type.

507

508 **References**

- 509 1. **Ulrich LE, Koonin E V, Zhulin IB.** One-component systems dominate signal  
510 transduction in prokaryotes. *Trends Microbiol* 2005;13:52–56.
- 511 2. **Cuthbertson L, Nodwell JR.** The TetR family of regulators. *Microbiol Mol Biol*  
512 *Rev* 2013;77:440–475.
- 513 3. **Manson JM, Keis S, Smith JMB, Cook GM.** Acquired bacitracin resistance in  
514 *Enterococcus faecalis* is mediated by an ABC transporter and a novel  
515 regulatory protein, BcrR. *Antimicrob Agents Chemother* 2004;48:3743–3748.
- 516 4. **Gauntlett JC, Gebhard S, Keis S, Manson JM, Pos KM, et al.** Molecular  
517 analysis of BcrR, a membrane-bound bacitracin sensor and DNA-binding  
518 protein from *Enterococcus faecalis*. *J Biol Chem* 2008;283:8591–8600.
- 519 5. **Gebhard S, Gaballa A, Helmann JD, Cook GM.** Direct stimulus perception  
520 and transcription activation by a membrane-bound DNA binding protein. *Mol*  
521 *Microbiol* 2009;73:482–491.
- 522 6. **Dintner S, Heermann R, Fang C, Jung K, Gebhard S.** A sensory complex  
523 consisting of an ATP-binding-cassette transporter and a two-component  
524 regulatory system controls bacitracin resistance in *Bacillus subtilis*. *J Biol*  
525 *Chem* 2014;289:27899–27910.
- 526 7. **Gebhard S, Fang C, Shaaly A, Leslie DJ, Weimar MR, et al.** Identification  
527 and characterization of a bacitracin resistance network in *Enterococcus*  
528 *faecalis*. *Antimicrob Agents Chemother* 2014;58:1425–1433.
- 529 8. **Ohki R, Giyanto, Tateno K, Masuyama W, Moriya S, et al.** The BceRS two-

530 component regulatory system induces expression of the bacitracin transporter,  
531 BceAB, in *Bacillus subtilis*. *Mol Microbiol* 2003;49:1135–1144.

532 9. **Bernard R, Guiseppi A, Chippaux M, Foglino M, Denizot F.** Resistance to  
533 bacitracin in *Bacillus subtilis*: Unexpected requirement of the BceAB ABC  
534 transporter in the control of expression of its own structural genes. *J Bacteriol*  
535 2007;189:8636–8642.

536 10. **Rietkötter E, Hoyer D, Mascher T.** Bacitracin sensing in *Bacillus subtilis*. *Mol*  
537 *Microbiol* 2008;68:768–785.

538 11. **Harwood S, Cutting C (eds).** *Molecular Biological methods for Bacillus*.  
539 Chichester, England: John Wiley & Sons, Inc.; 1990.

540 12. **Fang C, Stiegeler E, Cook GM, Mascher T, Gebhard S.** *Bacillus subtilis* as a  
541 platform for molecular characterisation of regulatory mechanisms of  
542 *Enterococcus faecalis* resistance against cell wall antibiotics. *PLoS One*  
543 2014;9:1–10.

544 13. **Patterson AG, Chang JT, Taylor C, Fineran PC.** Regulation of the Type I-F  
545 CRISPR-Cas system by CRP-cAMP and GalM controls spacer acquisition and  
546 interference. *Nucleic Acids Res* 2015;43:6038–6048.

547 14. **Ho SN, Hunt HD, Horton RM, Pullen JK, Pease LR.** Site-directed  
548 mutagenesis by overlap extension using the polymerase chain reaction. *Gene*  
549 1989;77:51–59.

550 15. **Nesterenko M V., Tilley M, Upton SJ.** A simple modification of Blum's silver  
551 stain method allows for 30 minute detection of proteins in polyacrylamide gels.  
552 *J Biochem Biophys Methods* 1994;28:239–242.



- 553 16. **Webb B, Sali A.** Comparative protein structure modeling using MODELLER.  
554 *Curr Protoc Bioinformatics* 2014;47:1–32.
- 555 17. **Radeck J, Kraft K, Bartels J, Cikovic T, Dürr F, et al.** The Bacillus BioBrick  
556 Box: generation and evaluation of essential genetic building blocks for  
557 standardized work with *Bacillus subtilis*. *J Biol Eng* 2013;7:29.
- 558 18. **Mondragón A, Subbiah S, Almo SC, Drottar M, Harrison SC.** Structure of  
559 the amino-terminal domain of phage 434 repressor at 2.0 Å resolution. *J Mol*  
560 *Biol* 1989;205:189–200.
- 561 19. **Sevilla-Sierra P, Otting G, Wüthrich K.** Determination of the nuclear  
562 magnetic resonance structure of the DNA-binding domain of the P22 c2  
563 repressor (1 to 76) in solution and comparison with the DNA-binding domain of  
564 the 434 repressor. *J Mol Biol* 1994;235:1003–1020.
- 565 20. **Pervushin K, Billeter M, Siegal G, Wüthrich K.** Structural role of a buried  
566 salt bridge in the 434 repressor DNA-binding domain. *J Mol Biol*  
567 1996;264:1002–1012.
- 568 21. **Harrison SC, Aggarwal AK.** DNA recognition by proteins with the helix-turn-  
569 helix motif. *Annu Rev Biochem* 1990;59:933–969.
- 570 22. **Bader MW, Sanowar S, Daley ME, Schneider AR, Cho U, et al.** Recognition  
571 of antimicrobial peptides by a bacterial sensor kinase. *Cell* 2005;122:461–472.
- 572 23. **Li M, Lai Y, Villaruz AE, Cha DJ, Sturdevant DE, et al.** Gram-positive three-  
573 component antimicrobial peptide-sensing system. *Proc Natl Acad Sci U S A*  
574 2007;104:9469–74.
- 575 24. **Otto M.** Bacterial sensing of antimicrobial peptides. *Contrib Microbiol*

2009;16:136–149.

25. **Economou NJ, Cocklin S, Loll PJ.** High-resolution crystal structure reveals molecular details of target recognition by bacitracin. *Proc Natl Acad Sci U S A* 2013;110:14207–12.
26. **Lyon GJ, Novick RP.** Peptide signaling in *Staphylococcus aureus* and other Gram-positive bacteria. *Peptides* 2004;25:1389–1403.
27. **Mascher T, Helmann JD, Uden G.** Stimulus perception in bacterial signal-transducing histidine kinases. *Microbiol Mol Biol Rev* 2006;70:910–938.
28. **Charlebois A, Jalbert LA, Harel J, Masson L, Archambault M.** Characterization of genes encoding for acquired bacitracin resistance in *Clostridium perfringens*. *PLoS One* 2012;7:e44449.

597

598 **Table 1. Identification of BcrR loss and gain of function point mutations**

Mutant No.	Domain	Base No.	Base change	AA change	Colour	Status	Frequency‡
BcrR8	DBD*	31	G-A	R11K	White	OFF	2
BcrR7	"	49	C-T	T17M	White	OFF	1
BcrR31	"	88	C-T	T30I	White	OFF	1
BcrR39	"	98	C-T	S33L	White	OFF	1
BcrR30	OGD <sup>#</sup>	124	C-T	P42L	White	OFF	3
BcrR17	"	151	C-T	S51F	White	OFF	3
					Blue/		
BcrR21	"	189	G-A	G64S	White	OFF	1
BcrR37	"	190	G-A	G64D	Blue	ON	2
BcrR10	TMD†	261	G-A	G88R	White	OFF	2
BcrR28	"	301	C-T	P101L	White	OFF	1
					Blue/		
BcrR18	"	367	C-T	T123I	White	OFF	1
BcrR1	"	421	G-A	G141D	White	OFF	1
BcrR16	"	534	G-A	E179K	White	OFF	2
					Blue/		
BcrR11	"	537	C-T	P180S	White	OFF	1
BcrR14	"	547	C-T	T183M	White	OFF	3

599

600 \*DBD DNA-binding domain; <sup>#</sup>OGD oligomerisation domain; †transmembrane domain;

601 ‡the number of times a point mutation was isolated.

602

603

604

605

606

607

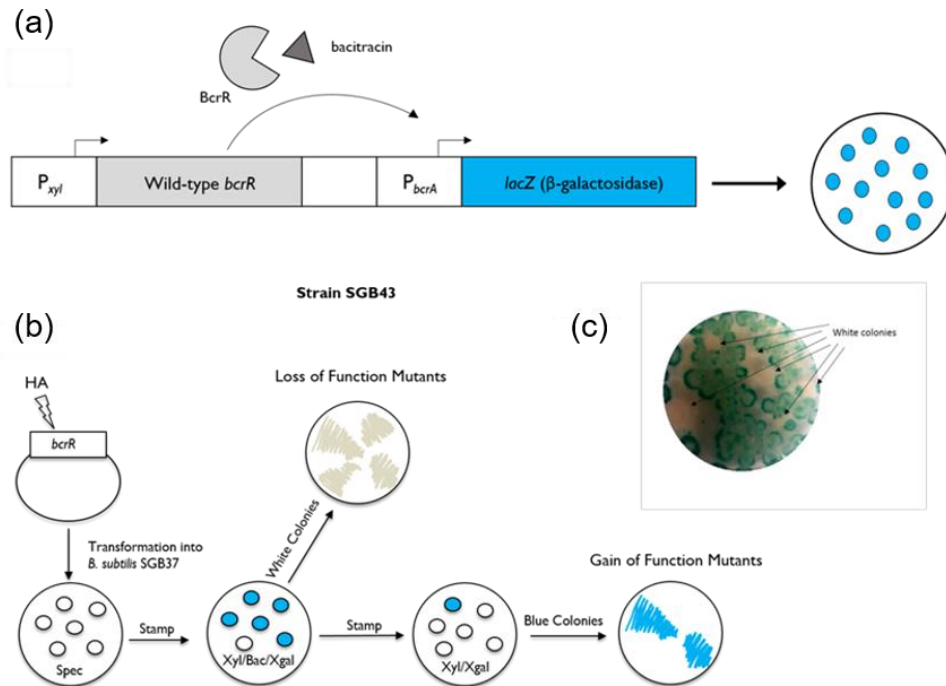


**Fig. 1. Identification of *bcrR* mutants using a  $\beta$ -galactosidase reporter ( $P_{bcrA}$ -*lacZ*).** Wild-type (WT) *bcrR* was cloned into the plasmid pXT under the xylose-inducible promoter to form pXT-*bcrR*. The *B. subtilis* strain SGB37 was transformed with pXT-*bcrR*, integrating upstream of the  $\beta$ -galactosidase reporter ( $P_{bcrA}$ -*lacZ*), to form the positive control strain SGB43 (a). In the positive control, WT BcrR is expressed and activated upon the addition of xylose (Xyl; 0.2%) and bacitracin (Bac; 0.5  $\mu\text{g ml}^{-1}$ ) respectively. Activated WT BcrR subsequently binds the  $P_{bcrA}$  promoter inducing expression of the  $\beta$ -galactosidase reporter, thereby producing blue colonies on LB agar plates containing Xgal (100  $\mu\text{g ml}^{-1}$ ) (a). In a separate experiment, pXT-BcrR plasmid DNA was mutagenised with hydroxylamine hydrochloride (HA), purified, and transformed into SGB37 (b). Transformants were plated on LB spectinomycin (spec) selection agar and the resulting colonies were subsequently stamped onto LB agar plates containing a combination of Xyl, Xgal, and Bac. This was used to screen for BcrR loss of function (LOF) and gain of function (GOF) mutants using a modified blue/white protocol [12]. In the presence of WT or GOF BcrR colonies were blue, while BcrR LOF mutants were white (b). Colonies from Xyl/Bac/Xgal plates were stamped on Xyl/Xgal only plates to select for blue GOF mutants (b and c).

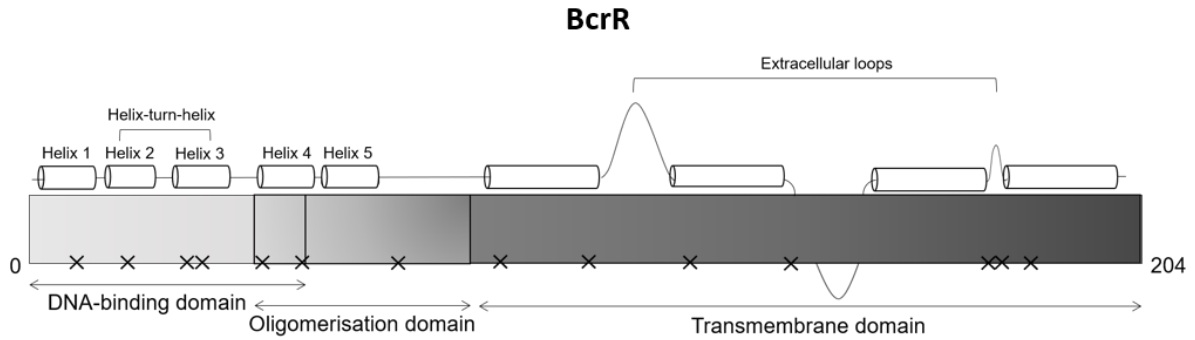


**Fig. 2. Mapping of LOF and GOF mutations on the BcrR protein.** BcrR is a 204 amino acid protein that consists of three putative functional domains: a N-terminal DNA-binding domain (light grey), an oligomerisation domain (medium grey), and a C-terminal transmembrane domain (dark grey). Loss and gain of function mutations (X) were mapped to the BcrR protein sequence to visualise the distribution of mutations.

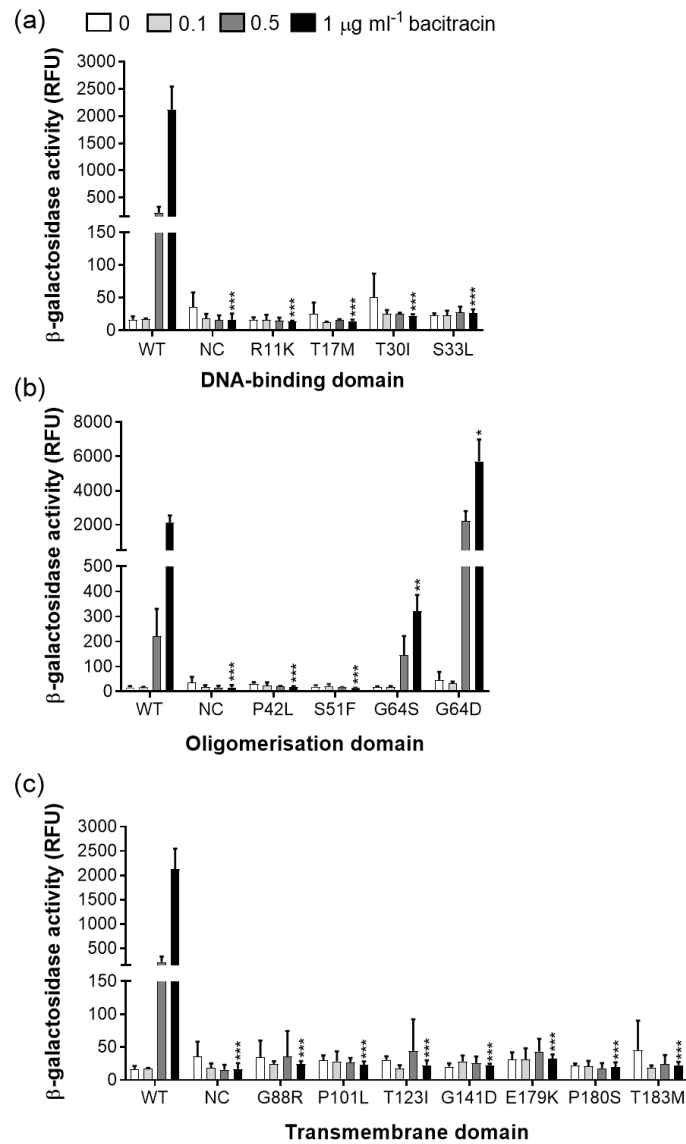


**Fig. 3. BcrR activity in response to bacitracin using a  $P_{bcrA}$ - $lacZ$  reporter.** Expression of the integrative  $P_{bcrA}$ - $lacZ$  promoter under the control of wild-type (WT) and mutant BcrR was measured using  $\beta$ -galactosidase activity. BcrR mutant activity is presented alongside WT and an empty vector negative control (NC) with data separated into putative functional domains: the DNA-binding domain (a), oligomerisation domain (b), and transmembrane domain (c). Data shown are the mean  $\pm$ SD ( $n$  = biological triplicate). Statistical significance was determined by performing an unpaired  $t$ -test of BcrR variants relative to WT at a bacitracin concentration of 1  $\mu$ g ml<sup>-1</sup> ( $p$  values: (\*) <0.05, (\*\*) <0.01, (\*\*\*) <0.005).

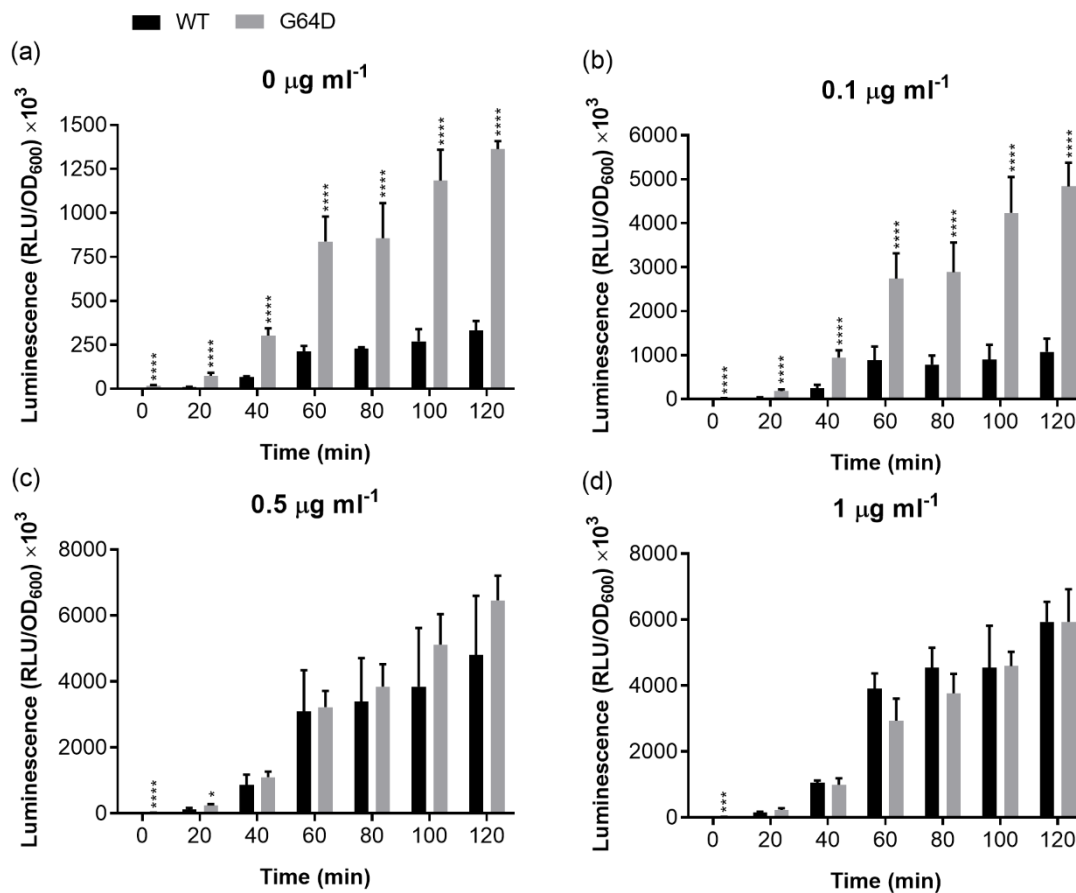


**Fig. 4. BcrR wild-type (WT) and G64D activity in response to bacitracin in the presence of xylose using the  $P_{bcrA}$ -*luxABCDE* reporter.** BcrR expression is controlled by a xylose-inducible promoter cloned upstream of the BcrR gene in the *B. subtilis* heterologous host. BcrR WT and G64D mutant activity was monitored under high (+ xylose) by measuring luciferase luminescence. WT and G64D BcrR activity were compared at bacitracin concentrations of 0, 0.1, 0.5, and 1 µg ml<sup>-1</sup> over a period of 120 min (a - d respectively). Data shown are the mean ± SD (*n* = biological quadruplicate). Statistical significance was determined by performing an unpaired *t*-test of G64D relative to WT (*p* values: (\*) <0.05, (\*\*) <0.01, (\*\*\*) <0.005, (\*\*\*\*) <0.001).

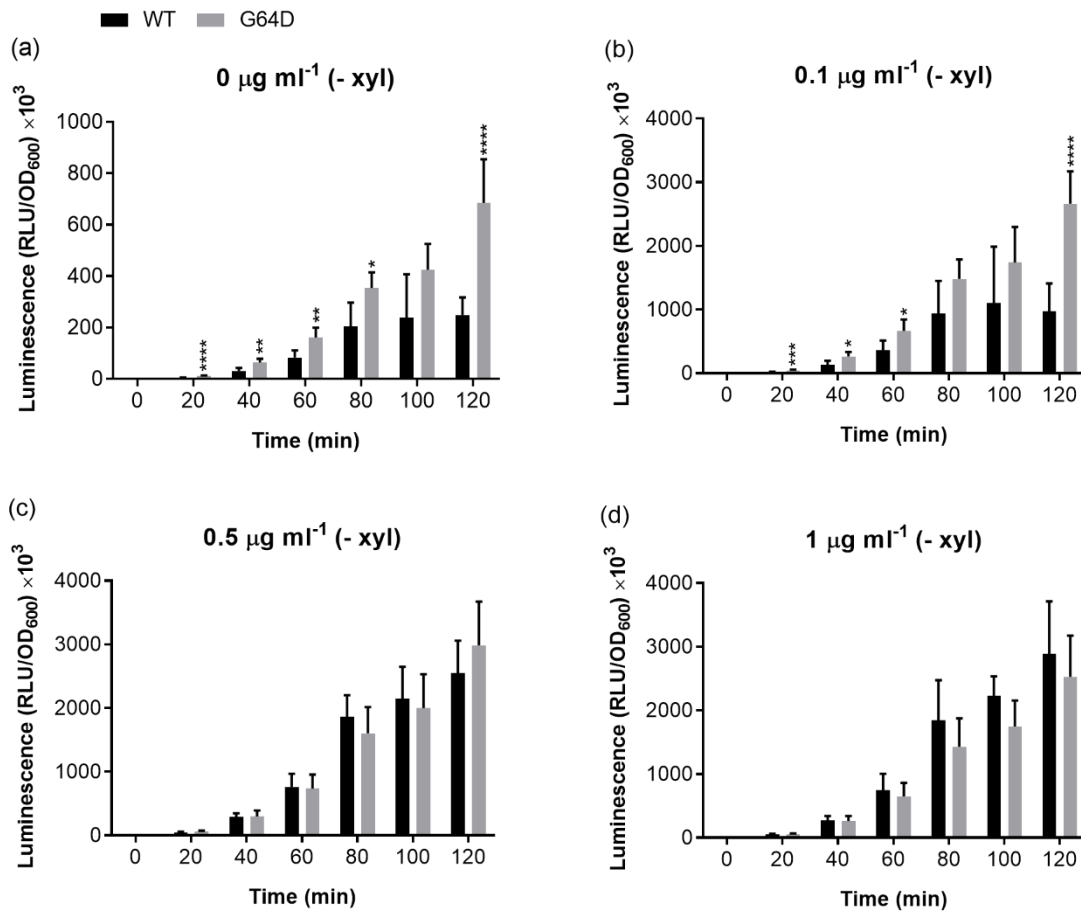


**Fig. 5. BcrR WT and G64D activity in response to bacitracin in the absence of xylose using the *P<sub>bcrA</sub>-luxABCDE* reporter.** BcrR WT and G64D mutant activity was monitored under low BcrR expression at bacitracin concentrations of 0, 0.1, 0.5 and 1 µg ml<sup>-1</sup> using a *P<sub>bcrA</sub>-luxABCDE* reporter (a – d). Activity was measured every 20 min for 120 min. Data shown are the mean ±SD (*n* = biological quadruplicate). Statistical significance was determined by performing an unpaired *t*-test of G64D relative to WT (*p* values: (\*) <0.05, (\*\*) <0.01, (\*\*\*) <0.005, (\*\*\*\*) <0.001).



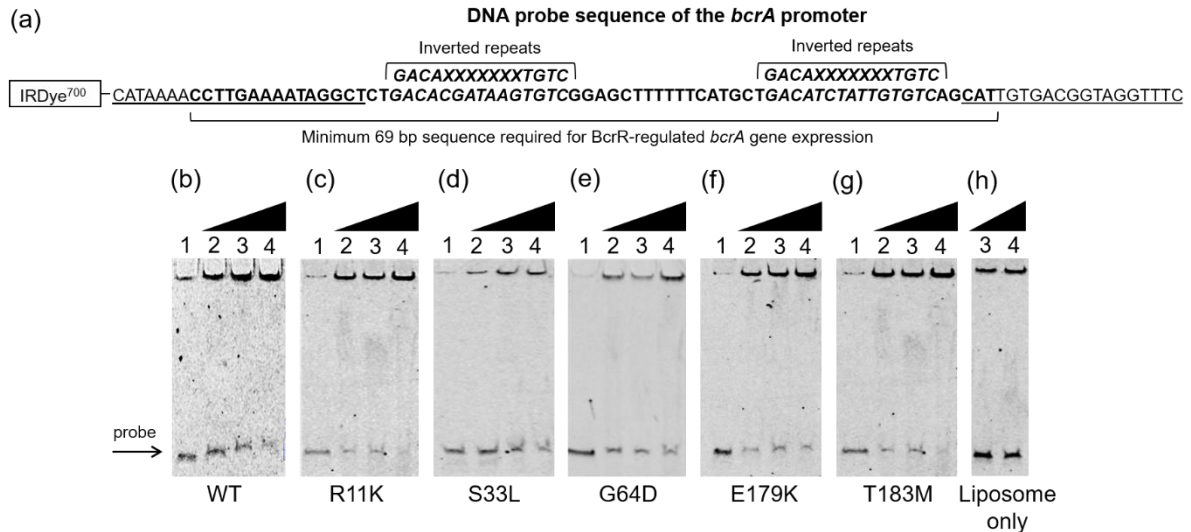


**Fig. 6. DNA-binding profiles of WT and mutant BcrR to  $P_{bcrA}$ .** (a) A 92 bp DNA probe ( $P_{bcrA}$ ) was amplified from the *bcrA* promoter sequence and labelled with a 5' fluorescent IRDye<sup>700</sup> tag for visualisation. This probe contained the 69 bp sequence (bold) necessary for *bcrA* expression, including the set of inverted repeats (bold and italicised) that are essential for BcrR DNA-binding [4,5]. The DNA-binding profiles of BcrR wild-type (WT) (b) and five BcrR mutants R11K (c), S33L (d), G64D (e), E179K (f), T183M (g) to the *bcrA* target promoter were compared using electrophoretic mobility shift assays.  $P_{bcrA}$  was incubated with BcrR WT and mutant proteoliposomes at protein: DNA molar ratios of 0:1 (lane 1), 25:1 (lane 2), 50:1 (lane 3), 125:1 (lane 4) the probe concentration.  $P_{bcrA}$  was shifted in a BcrR concentration-dependent manner in BcrR WT and all five mutants; no shift was observed in the absence of BcrR (lane 1) and no concentration-dependent shift was observed in the liposome only control (h). Lipid concentrations in lane 3 and 4 (h) are relative to lane 3 and 4 (b – g). Binding reactions were run on a 6% native PAGE gel at 350V for 25 min and visualised at 700 nm. The gels presented here are a representative of shifts that have been repeated at least three times.

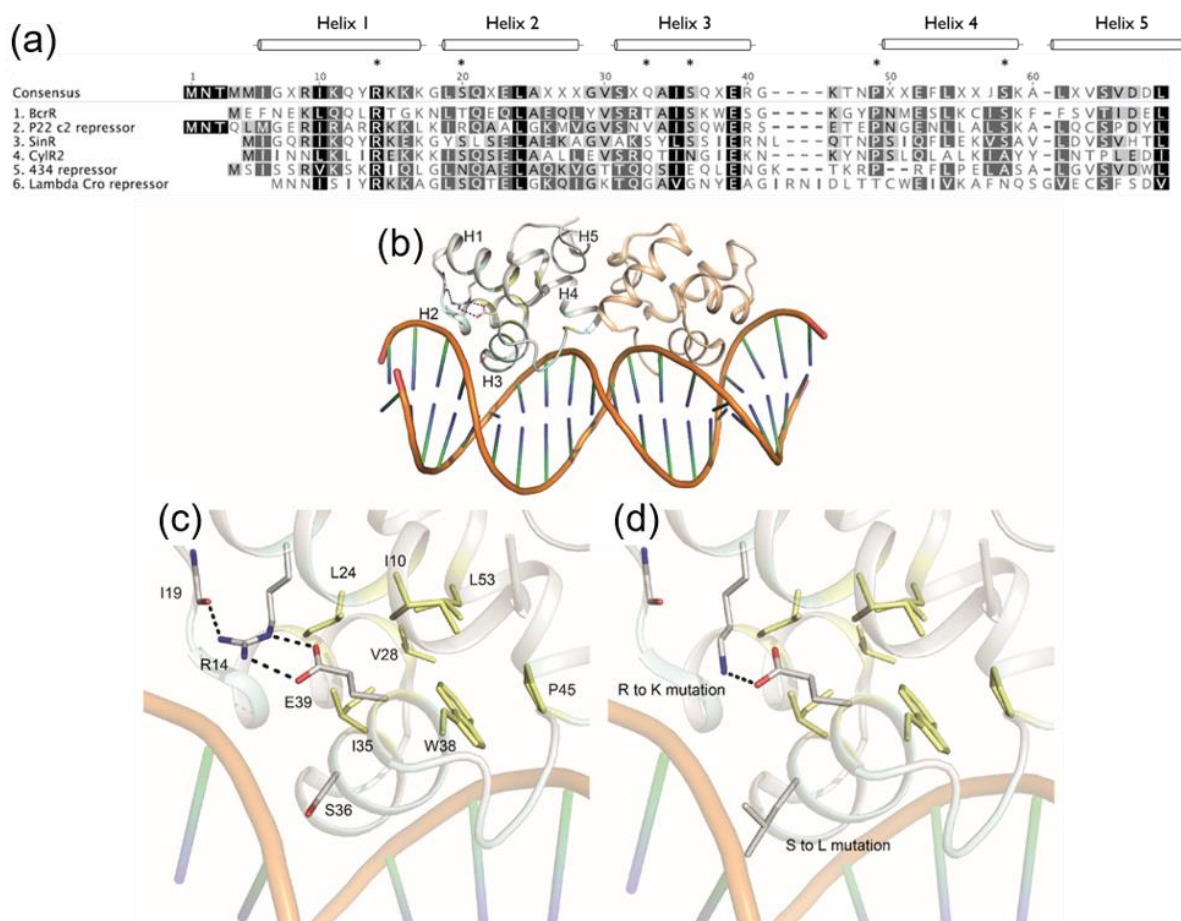


**Fig. 7. A three-dimensional model of the BcrR DNA-binding domain.** The BcrR DNA-binding domain sequence was aligned with five well-characterised XRE-type HTH DNA-binding proteins (a). The P22 c2 phage repressor protein had the highest sequence homology with the BcrR DNA-binding domain. The P22 c2 structure was used as a model in ProtMod for the structural analysis of the BcrR DNA-binding domain. The DNA-binding domain consists of five  $\alpha$  helices labelled 1-5 with helices 2 and 3 composing the HTH motif (b). Interactions between BcrR mutant residues, other residues in the DNA-binding domain, and the target DNA promoter sequence were analysed using PyMOL (c). DNA-binding domain wild-type (WT) residues were substituted with their mutant counterparts to observe consequential changes to their WT interactions (d - f).

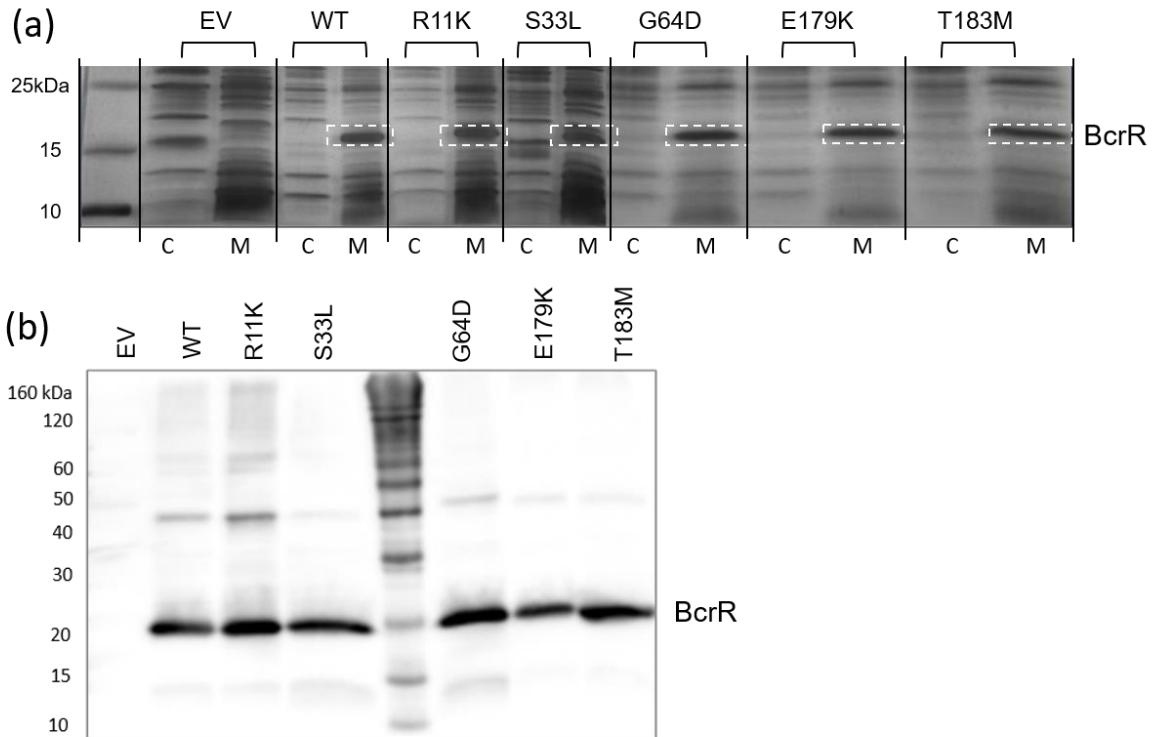


**Fig. 8. Localisation of BcrR WT and mutants to the cell membrane.** Cell cytosolic (C) and membrane (M) fractions of the empty vector control (EV), BcrR wild-type (WT), and mutants R11K, S33L, G64D, E179K, and T183M from the protein localisation experiment (about 200-500 µg total protein) were run on a 12.5% SDS-PAGE gel alongside a BenchMark™ His-tagged protein ladder (a). Membrane fractions were rerun on a 12.5% SDS-PAGE gel for Western Blot analysis. BcrR WT and mutant protein contained a His<sub>6</sub> C-terminal tag were subsequently probed for using an anti-His antibody. BcrR was detected in all membrane fractions, except the negative control (EV) (b).

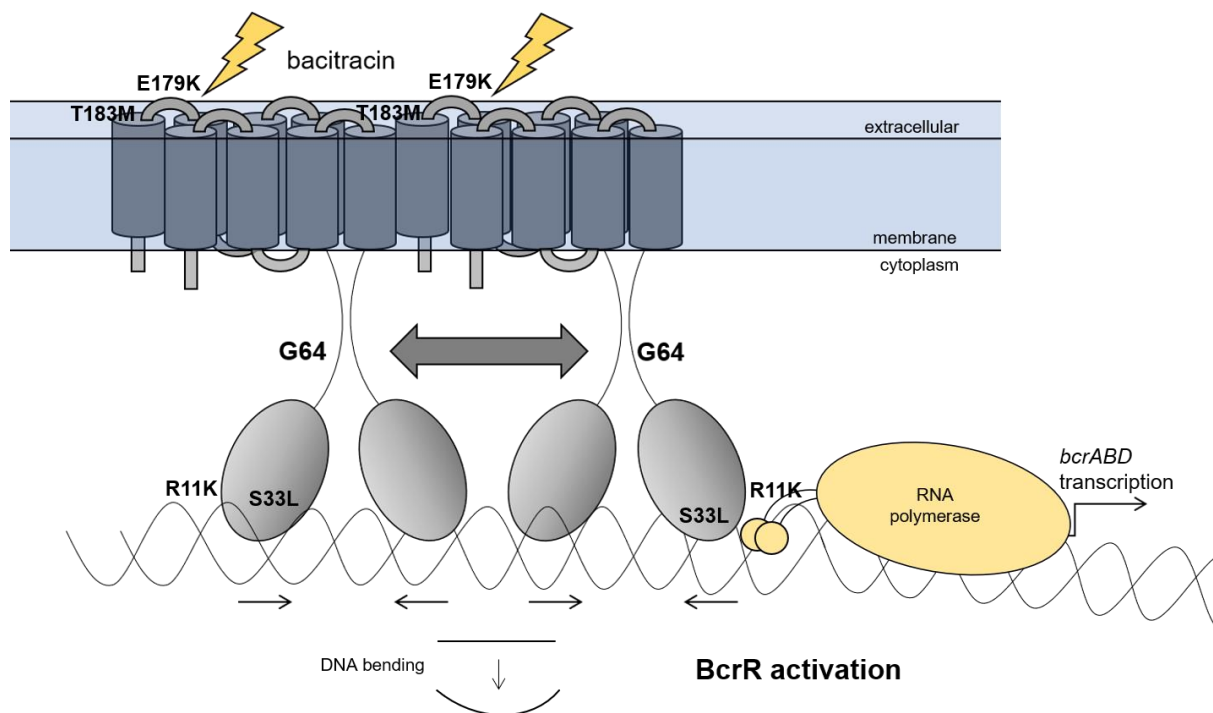


**Fig. 9. Schematic of bacitracin sensing and transcriptional activation by BcrR.** BcrR directly senses bacitracin and elicits a response through activation and subsequent initiation of *bcrABD* transcription. In this model BcrR detects bacitracin through a putative bacitracin-binding site localised to the second extracellular loop of the C-terminal transmembrane domain (E179K, P180S, and T183M). BcrR is constitutively bound to the *bcrA* promoter ( $P_{bcrA}$ ) but requires bacitracin for activation, likely through a conformational change, such as the oligomerisation of the BcrR dimers to form an active BcrR tetramer. Glycine 64 (G64) likely plays an essential role in this process. The BcrR DNA-binding domain contains five putative  $\alpha$  helices with a conserved XRE-type helix-turn-helix DNA-binding motif. R11 and S33 appear to have a crucial functional role in transducing the bacitracin activating signal to the DNA promoter. We hypothesise R11 and S33 are required for bacitracin-dependent changes in the local DNA topology, perhaps bending the DNA, to expose the binding site for RNA polymerase, allowing transcription of the *bcrABD* operon.

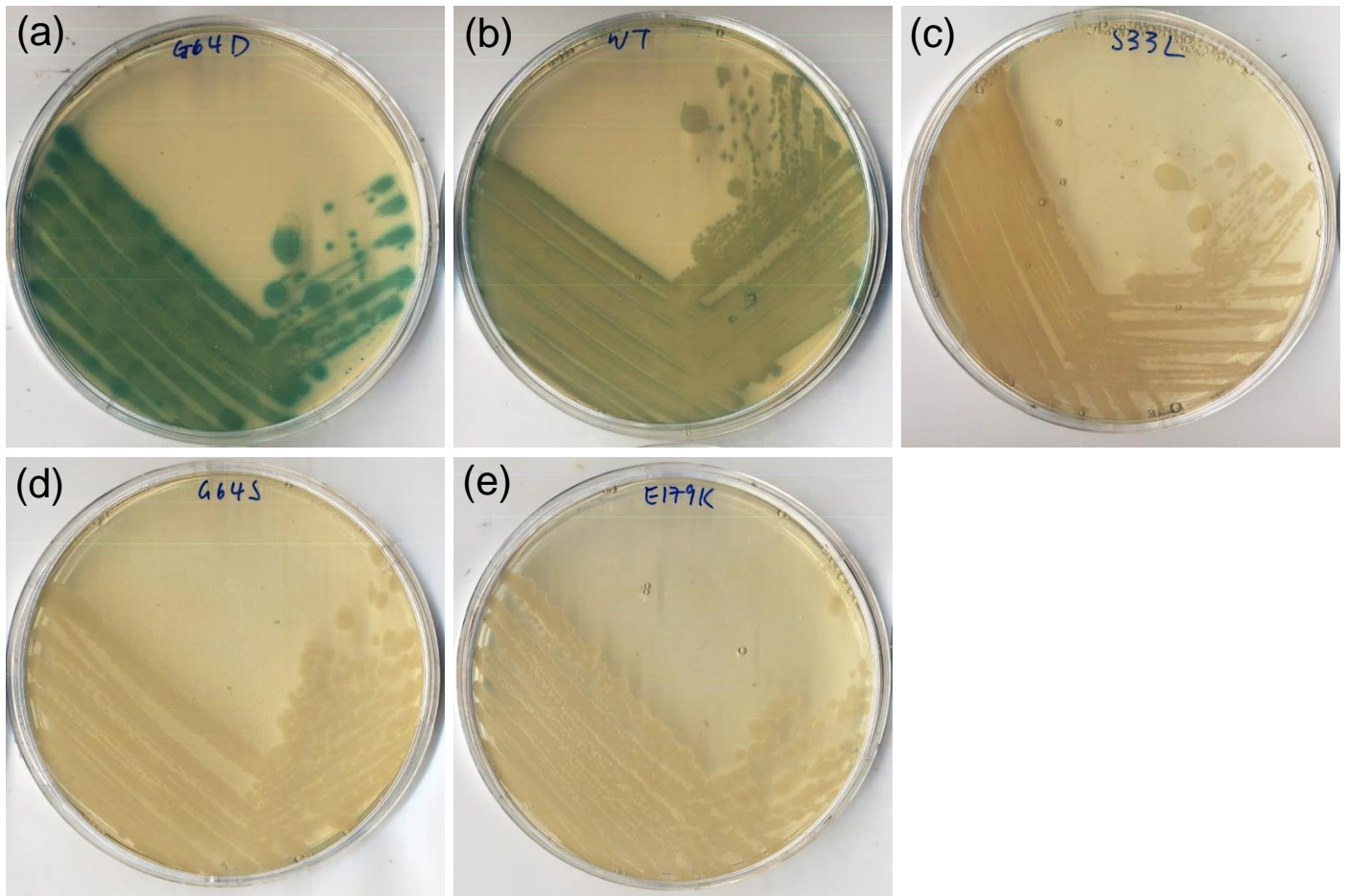


**Fig. S1. BcrR WT and mutant transformation into the  $P_{bcrA}$ -*lacZ* reporter strain *B. subtilis* SGB37.** Clonal cultures of the  $P_{bcrA}$ -*lacZ* reporter strain *B. subtilis* SGB37 were independently transformed with genomic DNA (gDNA) containing either the  $P_{xyl}$ -*bcrR* wild-type (WT) or mutant construct (S33L, G64S, G64D, and E179K). Transformants were plated on LB<sub>spec</sub> agar to select for gDNA containing the  $P_{xyl}$ -*bcrR* constructs. Three colonies were chosen for each *bcrR* variant and streaked onto LB<sub>xyl,bac,xgal</sub> agar and incubated at 37°C overnight. A representative photograph is presented here for each *bcrR* variant. The G64D gain of function mutant appears as blue colonies (a) which represents activated BcrR and are darker than the light blue WT colonies (b). The colonies of the loss of function mutants S33L (c), G64S (d), and E179K (e), appear white in colour, which represents a lack of active BcrR, i.e. loss of function.

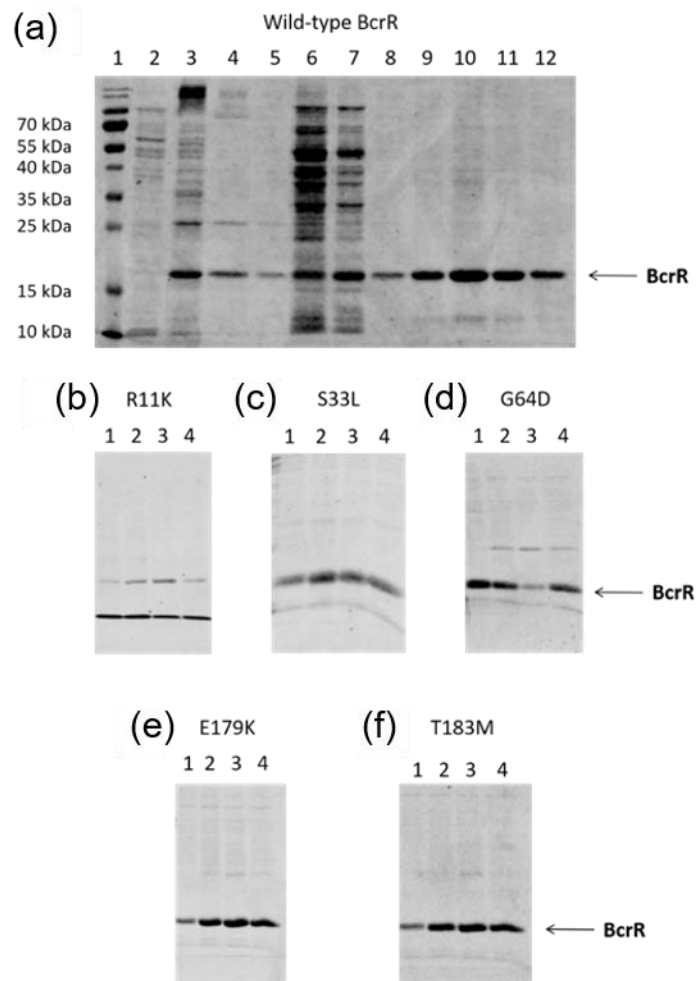


**Fig. S2. SDS-PAGE of purified wild-type (WT) and mutant BcrR protein.** BcrRHis protein was purified in a series of sequential steps. Samples were taken after each step and run on a 12.5% SDS-PAGE gel after purification. (a) Lane 2: supernatant from the sodium cholate wash to ensure BcrR was not removed from the membrane. Lanes 3,4,5: Sequential DDM solubilisation of BcrR. Lanes 6,7: protein fractions from the non-specifically bound protein. Lanes 8-12: protein fractions from the BcrR peak (these fractions were pooled for dialysis). (b - f) Lanes 1-3: purified BcrR fractions from the second purification peak for each of the BcrR mutants. Lane 4 (b - f): shows BcrR after fractions are pooled and dialysed. 10  $\mu$ l of sample were run regardless of total protein concentration (this equates to about 50  $\mu$ g in the purified protein lanes).



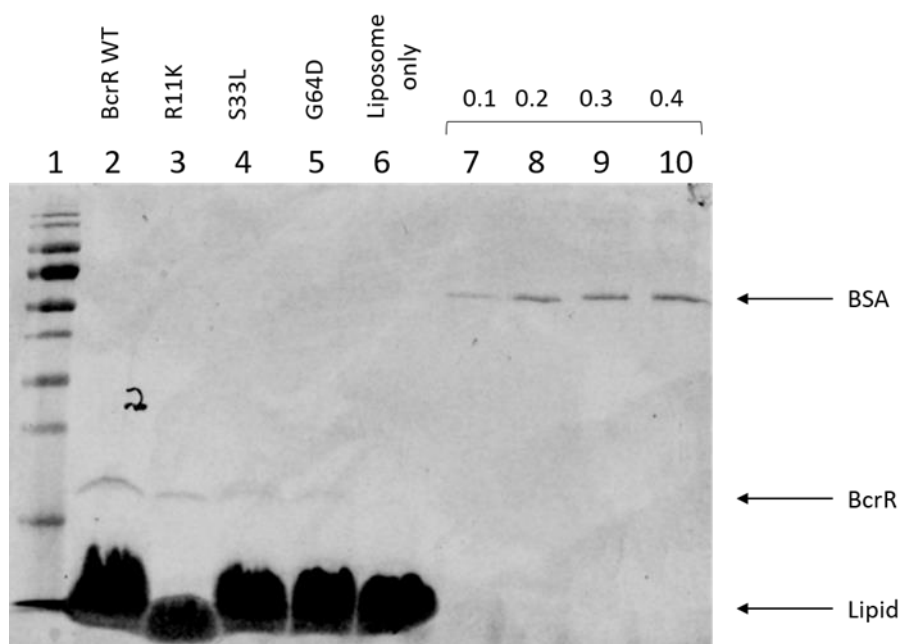


**Fig. S3. BcrR protein concentration in reconstituted liposomes by SDS-PAGE gel electrophoresis.** Wild-type (WT) BcrR protein and protein of BcrR mutants R11K, S33L, and G64D was purified and reconstituted into phosphatidyl choline liposomes. BcrR protein concentration in reconstituted proteoliposomes was determined by running 1.5  $\mu$ l of BcrR WT (2), R11K (3), S33L (4), and G64D (5) proteoliposome on a 4  $\times$  SDS-concentrated 12.5% SDS-PAGE gel against a BSA standard at a range of 0.1 - 0.4  $\text{mg ml}^{-1}$  (7 - 10). Protein size was determined by PageRuler™ protein ladder (1). A liposome only negative control was used to show absence of BcrR.

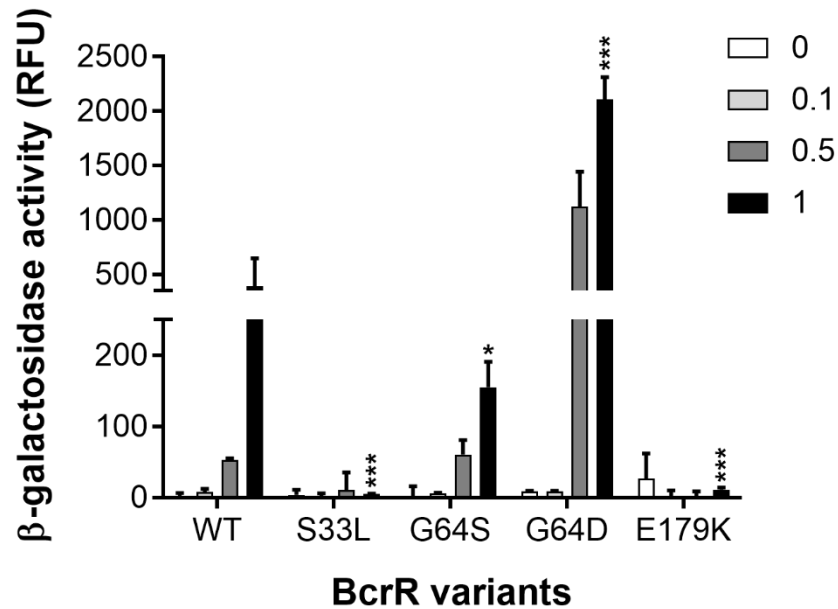


**Fig. S4. BcrR activity in response to bacitracin using a  $P_{bcrA}$ -*lacZ* reporter.** To confirm phenotypic observations of the new transformants, expression of the integrative  $P_{bcrA}$ -*lacZ* promoter under the control of wild-type (WT) and mutant BcrR was measured using  $\beta$ -galactosidase activity. BcrR mutant activity is presented alongside WT. Data shown are the mean  $\pm$ SD ( $n$  = biological triplicate). Statistical significance was determined by performing an unpaired  $t$ -test of BcrR variants relative to WT ( $p$  values: (\*)  $<0.05$ , (\*\*)  $<0.01$ , (\*\*\*)  $<0.005$ ).



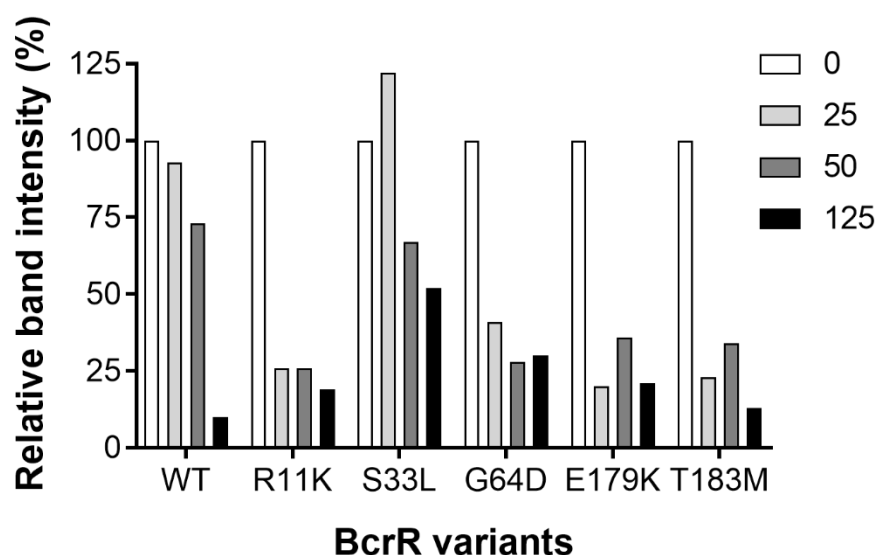


**Fig. S5. Densitometric analysis of the free probe in the electrophoretic mobility shift assays.**

Band intensities are expressed relative (%) to the probe only band (Fig. 6. lane 1 (b – g)) in each electrophoretic mobility shift assay for each BcrR variant. White bars, no BcrR proteoliposomes (Fig. 6. lane 1 (b – g)), light grey bars protein:DNA molar ratio of 25:1 (Fig. 6. lane 2 (b – g)), dark grey bars 50:1 (Fig. 6. lane 3 (b – g)), and black bars 125:1 (Fig. 6. lane 4 (b – g)).

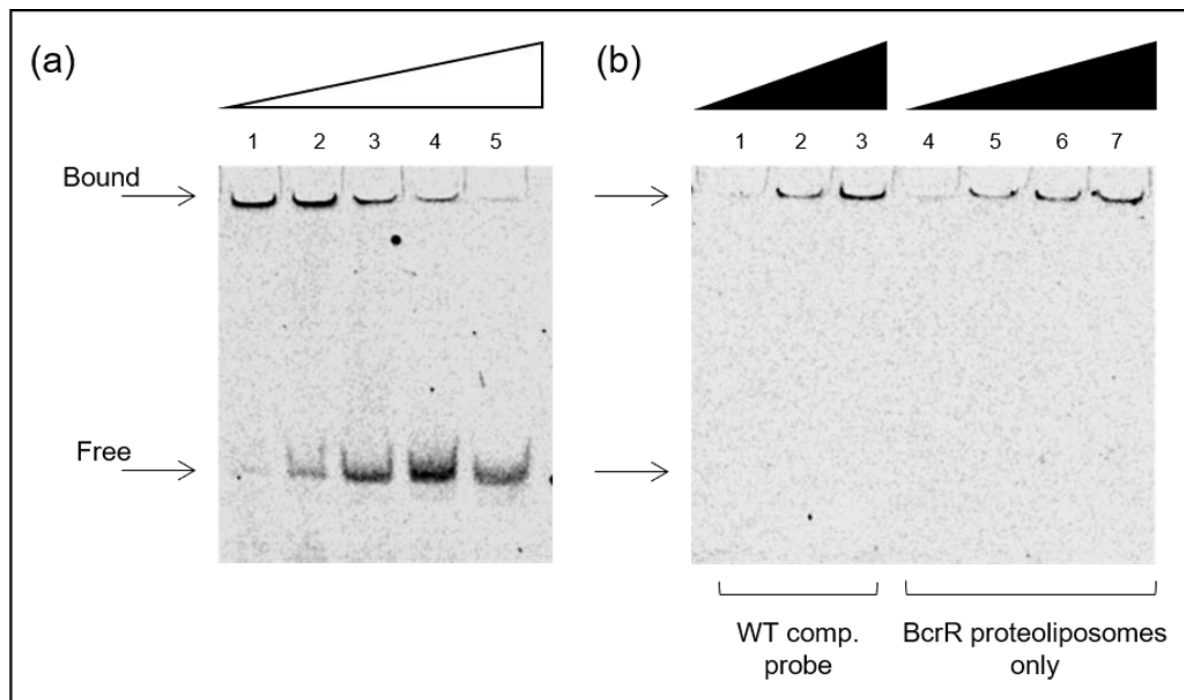


**Fig. S6. EMSA competition and controls for BcrR WT and  $P_{bcrA}$  target probe.** (a) Wild-type (WT) BcrR proteoliposomes (P/L) were incubated with a fluorescently labelled  $P_{bcrA}$  target probe and at increasing molar ratios of a non-labelled:labelled probe (5:1, 10:1, 20:1, 30:1, and 40:1) (lanes 1 – 5). The competitor probe was the same length and nucleotide sequence as the labelled target probe (see methods). Labelled probe and BcrR (proteoliposomes) were at a constant concentration of 1.25 ng and 400 ng, respectively. Fluorescently labelled bound probe was displaced at increasing concentrations concurrent with increasing non-labelled competitor probe. (b) Non-labelled competitor probe (1.25 ng) was incubated with increasing molar ratios of WT BcrR proteoliposomes (protein:DNA; 0:1, 50:1, and 125:1) (lanes 1 – 3). This confirmed the non-labelled competitor probe does not fluoresce. BcrR proteoliposomes only were shown to auto-fluoresce, with fluorescence increasing as liposome concentration increased (0, 100, 200, and 400 ng) (lanes 4 – 7). Binding reactions were incubated for 30 min at room temperature and then run on a 6% native PAGE gel at 350V for 25 min and visualised at 700 nm. Data presented here are a representative of shift assays that have been repeated at least three times.

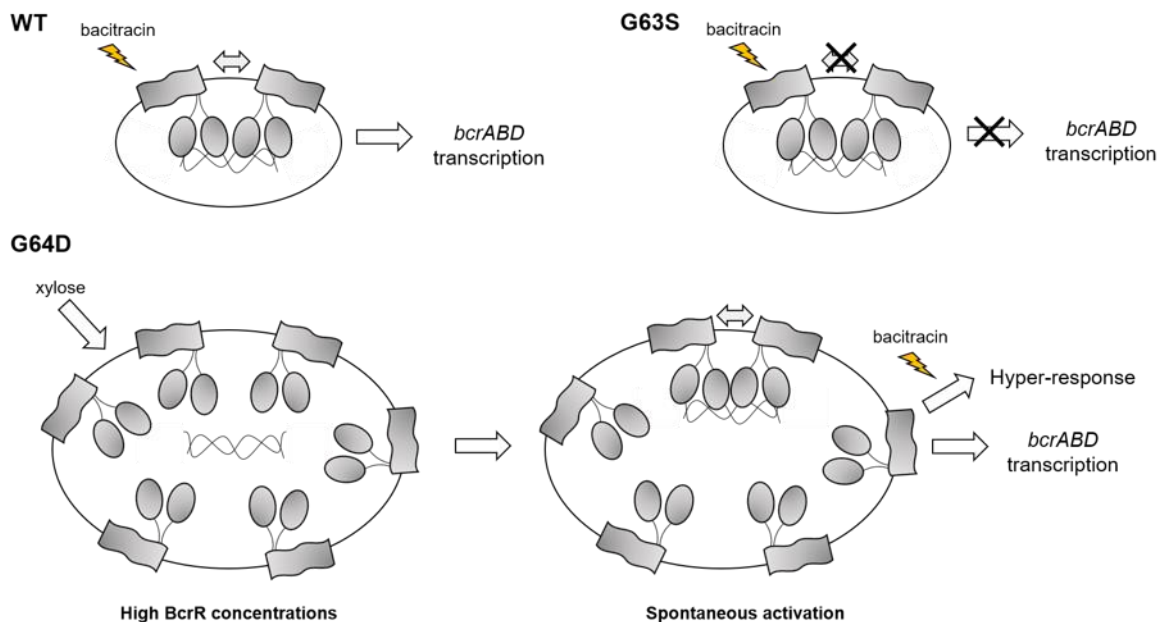


**Fig. S7. A proposed model of G64D activation.** Wild-type (WT) BcrR is constitutively bound to the *bcrA* target promoter but requires bacitracin for activation. BcrR gain of function mutant G64D can spontaneously activate and initiate expression from the *bcrA* promoter in the absence of bacitracin. This process relies upon high cellular concentrations of BcrR, as observed under a xylose-inducible promoter. In the presence of both xylose and bacitracin, G64D elicits a hyper-sensitive response as a result of spontaneous activation, in addition to bacitracin-induced activation. A G64S substitution results in a defective BcrR, unable to effectively elicit a response to bacitracin. This is likely due to an inability to oligomerise upon bacitracin-binding.

**Table S1. Bacterial strains and plasmids**

Strain or Plasmid	Description <sup>#</sup>	Reference/Source
<i>B. subtilis</i>		
SGB37	<i>bceAB::kan amyE::pES601(PbcrA-lacZ)</i> ; cm <sup>R</sup> kan <sup>R</sup>	[1]
SGB43	<i>bceAB::kan thrC::pES701(pXT-bcrR; E. faecalis)</i> <i>amyE::pES601(PbcrA-lacZ)</i> ; spec <sup>R</sup> cm <sup>R</sup> kan <sup>R</sup>	[1]
SGB273	TMB1518 <i>sacA::pNTlux101</i> ; cm <sup>R</sup>	[1]
SGB274	TMB1518 <i>thrC::pES701 sacA::pNTlux101</i> ; cm <sup>R</sup> spec <sup>R</sup>	[1]
BcrR_R11K	SGB37 harbouring pES701 BcrR <sup>R11K</sup> ; spec <sup>R</sup>	This study
BcrR_T17M	SGB37 harbouring pES701 BcrR <sup>T17M</sup> ; spec <sup>R</sup>	This study
BcrR_T30I	SGB37 harbouring pES701 BcrR <sup>T30I</sup> ; spec <sup>R</sup>	This study
BcrR_S33L	SGB37 harbouring pES701 BcrR <sup>S33L</sup> ; spec <sup>R</sup>	This study
BcrR_P42L	SGB37 harbouring pES701 BcrR <sup>P42L</sup> ; spec <sup>R</sup>	This study
BcrR_S51F	SGB37 harbouring pES701 BcrR <sup>S51F</sup> ; spec <sup>R</sup>	This study
BcrR_G64S	SGB37 harbouring pES701 BcrR <sup>G64S</sup> ; spec <sup>R</sup>	This study
BcrR_G64D	SGB37 harbouring pES701 BcrR <sup>G64D</sup> ; spec <sup>R</sup>	This study
BcrR_G88R	SGB37 harbouring pES701 BcrR <sup>G88R</sup> ; spec <sup>R</sup>	This study
BcrR_P101L	SGB37 harbouring pES701 BcrR <sup>P101L</sup> ; spec <sup>R</sup>	This study
BcrR_T123I	SGB37 harbouring pES701 BcrR <sup>T123I</sup> ; spec <sup>R</sup>	This study
BcrR_G141D	SGB37 harbouring pES701 BcrR <sup>G141D</sup> ; spec <sup>R</sup>	This study
BcrR_P180S	SGB37 harbouring pES701 BcrR <sup>P180S</sup> ; spec <sup>R</sup>	This study
BcrR_E179K	SGB37 harbouring pES701 BcrR <sup>E179K</sup> ; spec <sup>R</sup>	This study
BcrR_T183M	SGB37 harbouring pES701 BcrR <sup>T183M</sup> ; spec <sup>R</sup>	This study
BcrR_G64D_lux	SGB273 harbouring pES701 BcrR <sup>G64D</sup> ; spec <sup>R</sup>	This study

*E. coli*

DH10B	F- <i>mcrA</i> Δ( <i>mmr-hsdRMS-mcrBC</i> ) φ80 <i>dlacZ</i> Δ <i>M15</i> Δ <i>lacX74</i> <i>deoR</i>	[2]
C41(DE3)	<i>recA1 araD139</i> Δ( <i>ara leu</i> )7697 <i>galU galK rpsL endA1 nupG</i>	[3]
C41 pTrc99A	Uncharacterised mutant derivative from BL21(DE3)	This study
WT	C41(DE3) harbouring expression vector pTrc99A; <i>amp</i> <sup>R</sup>	This study
R11K	C41(DE3) harbouring pBcrRHis <sup>WT</sup> ; <i>amp</i> <sup>R</sup>	This study
S33L	C41(DE3) harbouring pBcrRHis <sup>R11K</sup> ; <i>amp</i> <sup>R</sup>	This study
G64D	C41(DE3) harbouring pBcrRHis <sup>S33L</sup> ; <i>amp</i> <sup>R</sup>	This study
E179K	C41(DE3) harbouring pBcrRHis <sup>G64D</sup> ; <i>amp</i> <sup>R</sup>	This study
T183M	C41(DE3) harbouring pBcrRHis <sup>E179K</sup> ; <i>amp</i> <sup>R</sup>	This study
	C41(DE3) harbouring pBcrRHis <sup>T183M</sup> ; <i>amp</i> <sup>R</sup>	This study

*E. faecalis*

AR01/DGVS	AR01/DG cured of pJM02 <i>bac</i> <sup>R</sup>	[4]
-----------	--	-----

*Plasmids*

pES701	pXT- <i>bcrR</i> (wild-type) <i>E. faecalis</i> ; <i>spec</i> <sup>R</sup>	[1]
pTrc99A	<i>E. coli</i> protein expression vector; <i>amp</i> <sup>R</sup>	[5]
pBcrRHis <sup>WT</sup>	pTrc99A- <i>bcrR</i> wild-type; <i>amp</i> <sup>R</sup>	This study
pBcrRHis <sup>R11K</sup>	pTrc99A- <i>bcrR</i> G33A mutation; <i>amp</i> <sup>R</sup>	This study
pBcrRHis <sup>S33L</sup>	pTrc99A- <i>bcrR</i> C98T mutation; <i>amp</i> <sup>R</sup>	This study
pBcrRHis <sup>G64D</sup>	pTrc99A- <i>bcrR</i> G192A mutation; <i>amp</i> <sup>R</sup>	This study
pBcrRHis <sup>E179K</sup>	pTrc99A- <i>bcrR</i> G535A mutation; <i>amp</i> <sup>R</sup>	This study
pBcrRHis <sup>T183M</sup>	pTrc99A- <i>bcrR</i> C548T mutation; <i>amp</i> <sup>R</sup>	This study

---

### Table S2. Primers used in this study

Name	Sequence 5'-3'	Used to amplify/create
pXT-check fwd	CCTTACCGCATTGAAGGCC	<i>bcrR</i>
pXT-check rev	GTATTCACGAACGAAAATCGCC	<i>bcrR</i>
BcrRFwd	AAATTTCCATGGAATTTAATGAAAAGCTACAA	BcrRHis <sup>WT</sup>
HisBcrRRev	AATTTGTCGACTTAGTGGTGGTGGTGGTGGTGTTCATTCCCATCTGCTT	"
BcrRR11KmutF	AACAGCTTA <u>A</u> GACTGGAAAGAACTTAACGCAGGAACAACCTT	BcrRHis <sup>R11K</sup>
BcrRR11KmutR	TTTCCAGTC <u>T</u> TAAGCTGTTGTAGCTTTTCATTAATTT	"
BcrRS33LmutF	CAGCCATTTT <u>T</u> AAAATGGGAAAGCGGCAAGGGTTACCCTAAC	BcrRHis <sup>S33L</sup>
BcrRS33LmutR	TCCCATTTTA <u>A</u> AATGGCTGTTCTTGATACATATAATTGCTC	"
BcrRG64DmutF	TACTATCGG <u>A</u> CGAAGAACTGATTACACTTGCCGAAACTGAA	BcrRHis <sup>G64D</sup>
BcrRG64DmutR	AGTTCTTCG <u>T</u> CCGATAGTAGTTCATCTATGGTCACAGAAAA	"
BcrRE179KmutF	CGGCAAGAA <u>A</u> AACCCTATATAACGGTACTTGTATTTTTTGCTG	BcrRHis <sup>E179K</sup>
BcrRE179KmutR	ATATAGGGTTT <u>T</u> TCTTGCCGCTAAAAACAGACAGCCAA	"
BcrRT183MmutF	CCTATATAA <u>T</u> GGTACTTGTATTTTTGCTGTTAATCGGCAAG	BcrRHis <sup>T183M</sup>
BcrRT183MmutR	ACAAGTACC <u>A</u> TTATATAGGGTTCTCTTGCCGCTGCAAAAAA	"
bcrA_EMSA_F	/5IRD700/CAT AAA ACC TTG AAA ATA GGC T	P <sub>bcrA</sub>
bcrA_EMSA_R	GAA ACC TAC CGT CAC AAT G	"

1. **Fang C, Stiegeler E, Cook GM, Mascher T, Gebhard S.** *Bacillus subtilis* as a platform for molecular characterisation of regulatory mechanisms of *Enterococcus faecalis* resistance against cell wall antibiotics. *PLoS One* 2014;9:1–10.
2. **Hanahan D, Jessee J, Bloom FR.** Plasmid transformation of *Escherichia coli* and other bacteria. *Methods Enzymol* 1991;204:63–113.
3. **Miroux B, Walker JE.** Over-production of proteins in *Escherichia coli*: Mutant hosts that allow synthesis of some membrane proteins and globular proteins at high levels. *J Mol Biol* 1996;260:289–298.
4. **Manson JM, Keis S, Smith JMB, Cook GM.** Acquired bacitracin resistance in *Enterococcus faecalis* is mediated by an ABC transporter and a novel regulatory protein, BcrR. *Antimicrob Agents Chemother* 2004;48:3743–3748.
5. **Amann E, Ochs B, Abel KJ.** Tightly regulated tac promoter vectors useful for the expression of unfused and fused proteins in *Escherichia coli*. *Gene* 1988;69:301–315.